



Estimating North American background ozone in U.S. surface air with two independent global models: Variability, uncertainties, and recommendations

The Harvard community has made this article openly available. [Please share](#) how this access benefits you. Your story matters

Citation	Fiore, A.M., J.T. Oberman, M.Y. Lin, L. Zhang, O.E. Clifton, D.J. Jacob, V. Naik, L.W. Horowitz, J.P. Pinto, and G.P. Milly. 2014. "Estimating North American Background Ozone in U.S. Surface Air with Two Independent Global Models: Variability, Uncertainties, and Recommendations." <i>Atmospheric Environment</i> 96 (October): 284–300. doi:10.1016/j.atmosenv.2014.07.045.
Published Version	doi:10.1016/j.atmosenv.2014.07.045
Citable link	http://nrs.harvard.edu/urn-3:HUL.InstRepos:34305999
Terms of Use	This article was downloaded from Harvard University's DASH repository, and is made available under the terms and conditions applicable to Open Access Policy Articles, as set forth at http://nrs.harvard.edu/urn-3:HUL.InstRepos:dash.current.terms-of-use#OAP

Estimating North American background ozone in U.S. surface air with two independent global models: Variability, uncertainties, and recommendations

A.M. Fiore^{a*}, J.T. Oberman^b, M. Lin^c, L. Zhang^{d,e}, O.E. Clifton^a, D.J. Jacob^d, V. Naik^f,
L.W. Horowitz^c, J.P. Pinto^g

^aDepartment of Earth and Environmental Sciences and Lamont-Doherty Earth Observatory, Columbia University, 61 Route 9W, Palisades, NY, USA; amfiore@ldeo.columbia.edu; oclifton@ldeo.columbia.edu

^bNelson Institute Center for Sustainability and the Global Environment (SAGE), University of Wisconsin-Madison, Madison, WI, USA; oberman.wisc@gmail.com

^cNOAA Geophysical Fluid Dynamics Laboratory and Atmospheric and Oceanic Sciences, Princeton University, 201 Forrestal Road, Princeton, NJ, USA; meiyun.lin@noaa.gov; larry.horowitz@noaa.gov

^dSchool of Engineering and Applied Sciences, Harvard University, 29 Oxford Street, Cambridge, MA, USA; djacob@fas.harvard.edu

^eDepartment of Atmospheric and Oceanic Sciences & Laboratory for Climate and Ocean-Atmosphere Studies, School of Physics, Peking University, China; zhanglg@pku.edu.cn

^fUCAR/NOAA Geophysical Fluid Dynamics Laboratory, Princeton, NJ, USA; Vaishali.Naik@noaa.gov

^gU.S. EPA, National Center for Environmental Assessment, Research Triangle Park, NC, USA; Pinto.Joseph@epa.gov

*Corresponding author; phone 1-845-365-8580; fax 1-845-365-8157

Keywords: surface ozone, background ozone, air pollution, air quality, exceptional events

Submitted to *Atmospheric Environment*

December 26, 2013

Abstract

Accurate estimates for North American background (NAB) ozone (O_3) in surface air over the United States are needed for setting and implementing an attainable national O_3 standard. These estimates rely on simulations with atmospheric chemistry-transport models that set North American anthropogenic emissions to zero, and to date have relied heavily on one global model. We examine, for the first time, NAB estimates for spring and summer 2006 with two independent global models (GEOS-Chem and GFDL AM3). Evaluation of the standard simulations, which include North American anthropogenic emissions, with mid-tropospheric O_3 retrieved from space and ground-level O_3 measurements, shows that the models often bracket the observed values, implying value in developing a multi-model approach to estimate NAB O_3 . Consistent with earlier studies, the models robustly simulate the largest nation-wide NAB levels at high-altitude western U.S. sites (average values of ~ 40 - 50 ppb in spring and ~ 25 - 40 ppb in summer) where it correlates with observed O_3 . At these sites, a 27-year GFDL AM3 simulation simulates observed O_3 events above 60 ppb and indicates a role for year-to-year variations in NAB O_3 in driving their frequency (contributing 50-60 ppb or more during some events). During summer over the eastern United States (EUS), when photochemical production from regional anthropogenic emissions peaks, NAB is largely uncorrelated with observed values and it is lower than at high-altitude sites (average values of ~ 20 - 30 ppb). We identify four processes that contribute substantially to model differences in specific regions and seasons: lightning NO_x , biogenic isoprene emissions and chemistry, wildfires, and stratosphere-to-troposphere transport. Differences in model representation of these processes contribute more to uncertainty in NAB estimates than the choice of horizontal resolution within a single model. We propose that future efforts seek to constrain these processes with targeted analysis of multi-model simulations evaluated with observations of O_3 and related species from multiple platforms, and thereby reduce the error on NAB estimates needed for air quality planning.

1. Introduction

The United States Environmental Protection Agency (U.S. EPA) sets National Ambient Air Quality Standards (NAAQS) to protect public health and environmental

welfare. Under the Clean Air Act, ground-level ozone (O_3) is regulated as a criteria air pollutant, with a review every five years to assess and incorporate the best available scientific evidence. Following these reviews, the threshold for the O_3 NAAQS has been lowered over the past decade, from 0.08 ppm in 1997 to the current threshold of 0.075 ppm (75 ppb) in 2008, with proposals calling for even lower thresholds, within a range of 60-70 ppb on the basis of the latest health evidence (Federal Register, 2010). In order to better understand how the O_3 NAAQS can most effectively be attained, a fundamental, quantitative understanding of the background O_3 – both magnitude and variability- over the United States is needed.

McDonald-Bueller et al. (2011) and the first draft of the current U.S. EPA Policy Assessment describe the relevance of background O_3 in the U.S. national O_3 standard-setting process. Here we review recent model estimates for background O_3 (Table 1) and, for the first time, compare simulations from two independent models (GEOS-Chem and GFDL AM3) in the context of observational constraints with a focus on spatial, seasonal, and daily variability. Differences between the models provide a first estimate of the error in our quantitative understanding. The type of process-oriented multi-model approach demonstrated here, tied closely to *in situ* and space-based observations, can harness the strengths of individual models to provide information requested by air quality managers during both the standard-setting and implementation processes.

The term “background” is ambiguous, with several definitions used in practice to estimate it from observations and models (e.g., see discussion in Fiore et al., 2003). The U.S. EPA defines a North American Background (NAB) as the O_3 levels that would exist in the absence of continental North American (i.e., Canadian, U.S., and Mexican) anthropogenic emissions (EPA, 2006). Background O_3 defined this way includes: natural O_3 produced photochemically from non-methane volatile organic compounds (NMVOC) and nitrogen oxides (NO_x) originating from biogenic emissions, wildfire effluents including NO_x , NMVOC and carbon monoxide (CO) originating from natural sources such as biogenic emissions from vegetation and wildfires; O_3 produced from precursor emissions outside of North America as well as global methane; and O_3 transported from the stratosphere. This definition restricts NAB to a model construct, estimated in simulations in which North American anthropogenic emissions are set to zero. The

desire to quantify the impact of Canadian and Mexican emissions on NAB O₃ has led to the term “U.S. background”, a parallel model construct but estimated by setting only U.S. anthropogenic emissions to zero.

The development of effective State Implementation Plans (SIPs), by which states demonstrate how non-attainment regions will reach compliance with the NAAQS, requires an accurate assessment of the role of local, regional, and background sources in contributing to individual high-O₃ events. The Clean Air Act includes a provision for ‘exceptional events’, whereby high-O₃ events due to natural causes (such as wildfires or stratospheric intrusions) or foreign influence (e.g., Asian pollution) can be exempted from counting towards non-attainment status (Federal Register, 2007). Modeling the specific components of NAB can provide information to aid in interpreting such events including attribution to specific sources.

In the previous review of the O₃ NAAQS, the U.S. EPA considered NAB estimates from the GEOS-Chem model for a single year (Fiore et al., 2003), the only estimates documented in the published literature at that time. Recent work has updated those estimates (Wang et al., 2009; Zhang et al., 2011) and compared them with NAB in regional models using GEOS-Chem boundary conditions (Emery et al., 2012; Mueller and Mallard, 2011) and considered additional years. The first NAB estimates with an independent global model, (GFDL AM3; hereafter AM3; Table 2) were found to episodically reach 60-75 ppb over the Western United States in spring (Lin et al., 2012a). By contrast, GEOS-Chem estimated a maximum NAB of 65 ppb (Zhang et al., 2011) and the AM3 NAB was typically ~10 ppb higher than GEOS-Chem NAB on days when observations exceeded 70 ppb (Lin et al., 2012a). These studies, however, focused on different simulation years. Here we examine the AM3 and GEOS-Chem NAB estimates in a fully consistent and process-oriented manner for the year 2006, drawing on a multi-decadal AM3 simulation to provide context for the single year inter-comparison. We include an evaluation of their base simulations with ground-based and space-based observations to identify conclusions that are robust to the specific modeling system, as well as situations where observation-based constraints can be most effective in reducing uncertainty.

2. Review of prior model estimates for NAB and its components

We focus here on model estimates for NAB using the U.S. EPA definition, which relies on simulations with North American anthropogenic emissions set to zero. Earlier reviews synthesize observations relevant for evaluating base model simulations at remote sites (McDonald-Buller et al., 2011; Reid et al., 2008; Vingarzan, 2004). Even with the same approach, model estimates will differ due to different representations of natural emissions and the choice of different years since meteorological variability alters the balance between transported vs. regionally produced O₃. In Table 1, we summarize published modeling studies that estimated various statistics for NAB, along with estimates from individual NAB sources (wildfires, lightning, stratospheric, global anthropogenic methane plus international anthropogenic emissions, and the sum of all natural sources).

Despite quantitative differences, a basic consensus emerges that the highest NAB levels generally occur during springtime and at western U.S. (WUS) high-altitude regions, with lowest NAB levels during EUS low-altitude regions in summer. The summertime minimum reflects the peak in regional photochemistry, which leads to accumulation of O₃ generated from regional precursors at the same time as it shortens the lifetime of O₃ mixing downward into the photochemically active boundary layer (see e.g., (Fiore et al., 2002)). At high-altitude WUS sites, models consistently indicate a correlation between NAB levels and total O₃ during spring (Emery et al., 2012; Fiore et al., 2003; Lin et al., 2012a; Lin et al., 2012b; Zhang et al., 2011), implying that enhanced NAB levels play a role in raising total O₃, including above the NAAQS threshold. While these results are qualitatively consistent across several modeling platforms, the models vary in their quantitative attributions for NAB and its specific sources.

A few studies report the annual fourth highest maximum daily average 8-hour (MDA8) NAB value, which represents the minimum threshold for an O₃ standard that would be achievable by eliminating all North American anthropogenic emissions. Consideration of different metrics, and different years complicates using the ranges across different modeling systems in Table 1 as error estimates. For example, mean values of NAB are unlikely to be static from year to year due to trends and variability in

both global anthropogenic emissions of O₃ precursors and natural sources of NAB. Indeed, a multi-model parameterization indicates an increase of ~4 ppb due to rising global CH₄ plus international anthropogenic emissions of non-methane O₃ precursors between 1960 and 2000 (Wild et al., 2012). More recent increases in Asian emissions may have additionally raised WUS NAB by up to 3 ppb in spring between 2001 and 2006 (Zhang et al., 2008). This Asian component of NAB, as well as European contributions and global anthropogenic methane has received particular attention under the UNECE Task Force on Hemispheric Transport of Air Pollution (Fiore et al., 2009; Reidmiller et al., 2009; TFHTAP, 2010; Wild et al., 2012). Recent studies have further documented the mechanisms by which Asian pollution can reach surface air over the WUS (e.g., (Brown-Steiner and Hess, 2011; Lin et al., 2012b).

Wang et al. (2009) additionally estimated summertime U.S. Background (USB) for 2001 conditions, including the influence of Canadian and Mexican anthropogenic emissions (excluding methane). They found that average USB is 4 ppb higher than NAB over the contiguous United States, and up to 33 ppb higher during transport events at U.S. border sites directly downwind of these sources. In the model, Canadian and Mexican sources often contributed more than 10 ppb to total surface O₃ in excess of the 75 ppb NAAQS threshold in eastern Michigan, western New York, New Jersey, and southern California (Wang et al., 2009).

The natural portion of NAB has been quantified in a few modeling studies and generally follows the same patterns as total NAB, with maximum levels occurring during spring at high-altitude regions of the WUS (Table 1). Natural sources of NAB can also contribute to high-O₃ events. Observational evidence indicates events mainly of stratospheric origin at high-altitude sites in the WUS (e.g., (Langford et al., 2009)) but these efforts are hampered by a sparse observational network. Models are useful for quantifying the frequency of these events and for determining the contribution of these events to seasonal mean ozone levels. For decades, quantifying the stratospheric contribution to the troposphere, and particularly to surface air, has been contentious, with controversy rooted in the imprecise methods for quantifying accurately this component, as summarized in Lin et al. (2012a) (see their Section 2.3). Lin et al. (2012a) demonstrate that stratospheric intrusions play an important role in driving variability,

including high-O₃ events, at high-altitude WUS sites during spring. High-altitude greatly increases susceptibility to stratospheric influence; for days when observed O₃ exceeds 70 ppb at monitoring sites in the western states of EPA Region 8 during April-June of 2010, Lin et al. (2012a) find that median values of stratospheric O₃ in the AM3 model are 10 ppb lower at the lower elevation AQS sites than at high-elevation sites. Episodic wildfires also contribute to high-O₃ events (*e.g.*, Jaffe and Wigder, 2012; McKeen et al., 2002; Mueller and Mallard, 2011), though Singh et al. (2010) found little O₃ production in wildfire plumes in California unless mixing with an urban plume occurred. The role of stratospheric intrusions and wildfires in contributing to differences between AM3 and GEOS-Chem high-NAB events is considered in Section 3.4.

3. North American background estimates from two independent global models

We compare background estimates for March through August of 2006 from two independent global models: the GEOS-Chem global chemistry-transport model (CTM) and the AM3 chemistry-climate model nudged to re-analysis winds. The models include different representations for the processes contributing to the abundance and distributions of tropospheric O₃ (Table 2). We evaluate the base O₃ simulations with hourly measurements from a ground-based network of monitoring sites and with monthly averaged retrievals from satellite instruments that are sensitive to O₃ in the mid-troposphere. We compare the models for March through August of 2006, the period analyzed previously by Zhang et al. (2011), drawing on the 27-year AM3 simulation to place the 2006 NAB estimates in the context of inter-annual variability. We note that the inter-annual variability may be underestimated in AM3 in some regions due its use of climatological inventories for soil NO_x and wildfire emissions.

3.1. Model NAB Simulations, Observations and Analysis Methods

Table 2 describes the model configurations for the GEOS-Chem and GFDL AM3 base simulations for the meteorological year 2006. The GEOS-Chem CTM has been applied in various configurations over the past decade to estimate NAB and its various components for the summer of 1995 (Fiore et al., 2002), the 2001 O₃ season (Fiore et al., 2003; Wang et al., 2009), and the 2006-2008 O₃ seasons (Zhang et al., 2011; Zhang et al.,

2013) including extensive evaluation with *in situ* and satellite observations. The AM3 model has previously been applied at ~50 km horizontal resolution globally to estimate the impacts of Asian pollution and stratospheric intrusions on surface O₃ over the WUS during March through June of 2010. Extensive evaluation with *in situ* and space-based observations for that period shows it represents the subsidence of Asian and stratospheric O₃ plumes over the WUS (Lin et al., 2012a; Lin et al., 2012b). The AM3 simulation used here is ~200 km horizontal resolution and is multi-decadal (1980-2007; first year is discarded as initialization), enabling us to place the year 2006 in the context of inter-annual variability (Section 4). Both models estimate NAB in U.S. surface air by setting North American anthropogenic emissions of aerosol and O₃ precursors to zero. Anthropogenic sources include fossil and biofuel combustion (including aircraft and ship emissions within the domain), agricultural waste burning, and fertilizer application.

For anthropogenic emissions inventories, GEOS-Chem uses the 2005 National Emissions Inventory for the U.S., while AM3 uses the historical ACCMIP emissions developed in support of IPCC AR5 (Lamarque et al., 2011; Lamarque et al., 2010). Differences in the North American anthropogenic emissions inventories (5.58 and 6.67 Tg N a⁻¹ in AM3 and GEOS-Chem, respectively; 4.85 and 5.32 Tg N a⁻¹ for the United States), while crucial to the standard simulation for comparison with observations, should be irrelevant for the NAB simulations. Shortcomings in model representation of anthropogenic emissions and isoprene chemistry do not necessarily preclude their use for examining NAB, particularly its daily to inter-annual variability driven by transported components of NAB, such as O₃ associated with stratospheric intrusions, production from lightning NO_x, wildfires, or methane.

The ground-based U.S. EPA Clean Air Status and Trends Network CASTNet site (CASTNet) were located to minimize the influence of polluted urban air (Baumgardner et al., 2002) and thus are useful for evaluating O₃ simulated by coarse grid models. Our evaluation focuses on the maximum daily 8-hour average (MDA8) O₃ concentrations, the statistic currently used by the U.S. EPA to assess compliance with the O₃ NAAQS (a location is considered to be in violation of the NAAQS when the three-year-average of the fourth highest MDA8 exceeds the current 75 ppb threshold). Simulated MDA8 is calculated from archived hourly average O₃ concentrations in the model surface layer.

All statistics are calculated by sampling the models at the locations of CASTNet sites with bilinear interpolation from the four nearest model grid cells to the latitude and longitude at each station.

Columns retrieved from satellite instruments are sensitive to free tropospheric O₃ and enable an evaluation on a continuous spatial scale of the simulated background available to subside into surface air. We use here direct tropospheric O₃ retrievals from both the Ozone Monitoring Instrument (OMI) (Liu et al., 2010) and the Tropospheric Emission Spectrometer (TES) (Beer, 2006). All data are processed using a single fixed a priori as described in Zhang et al. (2010). Previous validation of these retrievals against *in situ* and aircraft measurements indicate an accuracy to within 5 ppb at 500 hPa (Zhang et al., 2010) and references therein). We remove the average bias of the satellite columns as compared to sondes at northern mid-latitudes prior to comparing with the model mid-tropospheric O₃ distributions and apply the appropriate satellite averaging kernels to the model daily ozone fields for direct comparison with the retrieved satellite O₃ columns (Zhang et al., 2010).

3.2 Regional and seasonal NAB estimates

Seasonal mean MDA8 NAB O₃ is consistently higher over the WUS than the EUS in both models (Figure 1). During spring, AM3 simulates higher NAB over the high-altitude Western U.S., which we attribute at least partially to a larger stratospheric influence in AM3 (Lin et al., 2012a) than in GEOS-Chem (Zhang et al., 2011). It is not clear whether AM3 actually simulates more stratosphere-to-troposphere exchange of O₃, or whether it mixes free tropospheric air (including the stratospheric component) into the planetary boundary layer more efficiently. Evaluation with daily O₃ sondes will be important to ascertain whether the models represent the vertical structure of O₃ throughout the troposphere and lower stratosphere, as shown for AM3 during the 2010 CalNex field campaign (Lin et al., 2012a; Lin et al., 2012b). During summer, the different simulated spatial patterns for NAB over the western U.S. are influenced by differences in the lightning NO_x sources as discussed further in Section 3.4.3.

Figure 2 shows the spatial patterns of the fourth highest NAB value between March 1 and August 31. As the ozone seasonal cycle is typically highest during the

summer in polluted regions, we expect the fourth highest during this six-month period to represent reasonably this statistic over a full year. AM3 simulates the highest values over Colorado whereas GEOS-Chem indicates that the highest values occur over New Mexico (Figure 2), reflecting the excessive NAB produced from lightning NO_x (Zhang et al., 2013). Due to different seasonal timing of these processes, AM3 simulates the fourth highest values during spring over much of Colorado but GEOS-Chem simulates peak values over much of New Mexico during August (Figure 2). Over Minnesota and Wisconsin, GEOS-Chem generally produces the fourth highest values in spring but AM3 suggests they occur in summer. The fourth highest values often occur during months when model biases are largest (Section 3.4), indicating that bias-correction techniques may be necessary for quantitatively accurate NAB estimates at specific locations and times. Over the northeastern states and west coast, the fourth highest values generally occur during spring, though later dates occur in the southeastern states, with occurrences generally later in GEOS-Chem than AM3. In the following sections, we analyze the model NAB estimates in the context of evaluating the total surface O_3 simulations with both space- and ground-based observations, a first step towards developing the process-level knowledge needed for accurate bias-correction.

3.3 Constraints from space-based observations

With the exception of O_3 produced within the U.S. boundary layer from CH_4 or natural NMVOC and natural NO_x , NAB in surface air mixes downward from the free troposphere. We use 500 hPa products retrieved from both the OMI and TES instruments aboard the NASA Aura satellite to evaluate the potential for space-based constraints on simulated mid-tropospheric O_3 distributions and thus the reservoir of mid-tropospheric O_3 , which includes NAB, available to mix downward into surface air. Biases relative to northern mid-latitude O_3 sondes (Zhang et al., 2010) have been uniformly subtracted from the retrieved products prior to the comparison with AM3 and GEOS-Chem shown in Figures 3 and 4. As evident from Zhang et al. (2010; see their Figure 5), the bias is not uniform and thus the real model error may deviate at any particular location from the true O_3 abundance differently than implied by the comparison with the satellite products reported here.

During spring, AM3 estimates a stronger north-to-south O₃ decrease in the mid-troposphere than GEOS-Chem (Figure 3). The satellite retrievals from both instruments suggest a stronger gradient than simulated with GEOS-Chem, which generally underestimates O₃ in the northern half of the United States compared both to TES (5-15 ppb) and OMI (up to 10 ppb). In contrast, AM3 mid-tropospheric O₃ is higher than the satellite products in the northern half of the domain, with a closer match to the OMI retrievals (generally within 5 ppb over the United States) than TES (positive biases up to 10-20 ppb). Prior direct evaluation of AM3 with O₃ sondes indicates biases of up to 10 ppb in AM3 at the high northern latitude sites of Alert and Resolute at 500 and 800 hPa with little bias in spring at the mid-latitude North American sites of Edmonton, Trinidad Head, Boulder and Wallops Island (Naik et al., 2013), roughly consistent with the biases relative to OMI.

Both satellite instruments indicate a general decrease from spring into summer over the western and northern United States, but an increase over several southeastern states, northern Mexico, and the Gulf of Mexico (compare Figures 3 and 4). The summertime spatial pattern of U.S. O₃ observed from space is broadly consistent with that estimated by interpolating upper tropospheric ozonesonde measurements during August of 2006 (Cooper et al., 2007). While the increases from spring to summer in the mid-troposphere over the EUS may include a contribution from lofting of regional anthropogenic O₃ production, there is likely also a contribution from the larger lightning NO_x source in the free troposphere during summer. GEOS-Chem estimates a summertime mid-tropospheric O₃ enhancement at mid-latitudes, centered over the United States whereas AM3 simulates a gradient with O₃ generally increasing along the southwest-to-northeast direction (Figure 4). The AM3 model tends to be high in summer by up to 15-20 ppb compared to both retrievals over Canada, as for the springtime comparison with TES, but with larger biases than in spring compared to OMI.

We expect discrepancies between AM3 and observations during summer in forested boreal regions due to the use of a climatological wildfire inventory and the vertical distribution used to prescribe those emissions (Dentener et al., 2006), which lofts fire effluents into the mid-troposphere where they can efficiently produce O₃ and PAN (see also Section 3.4.2). GEOS-Chem includes fire emissions representative of the year

2006 and restricts emission to the planetary boundary layer, and the mid-tropospheric O₃ biases versus the satellite products are smaller than AM3 in this region. The model differences in mid-tropospheric O₃ distributions shown in Figures 3 and 4 likely contribute to the different spatial distributions of simulated NAB at the surface, specifically the higher NAB estimated with AM3 over the northern United States and Canada relative to the NAB estimated with GEOS-Chem (Figures 1 and 2).

In both Figures 3 and 4, the models are generally more consistent with the OMI retrievals, which likely reflect differences in the vertical sensitivity of the TES and OMI instruments. While the satellite retrievals provide useful qualitative constraints on the simulated mid-tropospheric distributions, the disagreement between OMI and TES over many locations (grey boxes in Figures 3 and 4) hinders their quantitative utility. The higher sampling frequency possible from instruments on geostationary satellites such as TEMPO (Hilsenrath and Chance, 2013) should improve the potential for space-based constraints on free-tropospheric and near-surface distributions.

We can nevertheless glean additional insights into the model vertical distributions of NAB by examining differences in the models sampled with the two different averaging kernels. For example, over Canada, GEOS-Chem indicates that OMI would measure higher O₃ than TES whereas AM3 indicates that TES should retrieve higher O₃ than OMI during both seasons. In the spring, the retrieved OMI product is generally higher than TES over this region, as simulated by AM3. GEOS-Chem is generally within 10 ppb of the OMI product with a tendency to underestimate springtime mid-tropospheric O₃ over Canada, whereas AM3 is generally within 5 ppb of OMI over much of the United States, with a tendency towards a positive bias. During summer, TES is higher than OMI over Canada. The high O₃ bias over the EUS in AM3 is confined close to the surface (Figure 5) since AM3 tends to underestimate free tropospheric O₃, particularly over the convectively active Gulf of Mexico region where lightning NO_x is expected to be an important source of NAB O₃. We conclude that the estimates from the models could bracket the true NAB in many cases, but the ability of the models to bracket the satellite measurements does not preclude biases in the NAB estimates. This conclusion is examined further below by comparisons of the two models with ground-based measurements.

3.4 Constraints from ground-based measurements

We use the CASTNet MDA8 O₃ observations to further constrain the model NAB estimates through an evaluation of the base simulations, which include all anthropogenic emissions, to simulate total surface O₃. Since NAB depends strongly on altitude (Figure 1; references in Table 1), the remainder of our analysis separates the data by altitude to gain insight into the different processes shaping NAB distributions. Specifically, we divide the CASTNet sites into two groups: (1) below 1.5 km in elevation (low-altitude sites), primarily sites in the EUS, and (2) Intermountain West CASTNet sites with elevation greater than 1.5 km (high-altitude sites). This second category includes all high-altitude CASTNet sites except for those in California.

3.4.1. Seasonal Variability

Figure 5 shows the observed and simulated seasonal cycles at the CASTNet sites. At the high-altitude sites, both models are generally within 5 ppb of the regional mean observed values and usually fall within one standard deviation of the observed monthly mean values at the sites within the region. Consistent with the evaluation in Section 3.3, the models tend to bracket the observations, but with notably different seasonal cycles. AM3 peaks in early spring, overestimating observed values in March but then declines to slightly underestimate observed values in June and July. In contrast, GEOS-Chem underestimates observed values from March through July but increases to overestimate observed values in August. The model differences are amplified in the NAB estimates: AM3 simulates a large seasonal decline in NAB from springtime (near 50 ppb) into summer (below 35 ppb) while GEOS-Chem estimates little seasonality in NAB (monthly mean values around 40 ppb).

At the low-altitude sites, AM3 exhibits a large positive bias in total surface O₃ in all months, most problematic during summer. The exacerbation of the bias in summer implies a problem with O₃ produced from regional emissions, with isoprene-NO_x-O₃ chemistry a likely culprit given its different treatment in the models (Table 2; see Section 3.5.3). Both models show declining NAB levels from spring into summer, though the GEOS-Chem amplitude of the seasonal cycle is smaller than that of AM3. The AM3

discrepancy with observations is much larger than the difference between the GEOS-Chem and AM3 NAB estimates except for March and April. If we focus on March and April, and assume that the model biases at both the high and low altitude sites are entirely due to problems representing NAB, then the models would be more consistent in their NAB estimates. While we conclude that the AM3 NAB at low-altitude sites is too high in March since we expect NAB to be lower than the observed value, it is possible that NAB could actually be higher in an atmosphere with lower NO_x than under current conditions due to more efficient O_3 production and slower chemical loss.

At the high-altitude sites in summer, the GEOS-Chem overestimate of observed O_3 has been attributed previously to an overestimate of O_3 produced from lightning NO_x when prescribing a higher production of NO_x from flashes at mid-latitudes and spatially scaling the source to match LIS-OTD climatological flash counts (Murray et al., 2012), which may lead to regional errors for a specific year (Zhang et al., 2013). The larger difference between the NAB estimates from the two models in August than between the simulated and observed total O_3 implies that the agreement with observations, while a necessary condition, does not sufficiently constrain the NAB estimates.

3.4.2. Daily Variability

Figure 6 shows probability density distributions constructed from observed and simulated MDA8 O_3 in spring (top) and summer (bottom) sampled at the high-altitude (left) versus low-altitude (right) CASTNet sites, and statistics are summarized for the AM3 and high-resolution GEOS-Chem simulations in Table 3. We additionally include in Figure 6 estimates from a coarse resolution version of the GEOS-Chem model (green) in order to examine the extent to which differences in horizontal resolution contribute to the different NAB and total O_3 estimates in AM3 versus GEOS-Chem. In all cases, the NAB (dotted lines) differ more between the GEOS-Chem and AM3 models than between the high- versus low-resolution versions of GEOS-Chem. This conclusion also holds for the total O_3 distributions in spring. In summer, however, the total O_3 distributions in GEOS-Chem are more sensitive to the choice of horizontal resolution, presumably reflecting the larger contributions from local-to-regional photochemical production during this season and the importance of spatially resolving domestic anthropogenic and

natural emissions distributions. Emery et al. (2012) found that the higher resolution CAMx model generally simulated higher WUS NAB than a coarse resolution version of GEOS-Chem, and better agreement has been noted between CAMx and the higher resolution version of GEOS-Chem (EPA, 2013). Simulation of higher WUS NAB by higher resolution models (Emery et al., 2012; Lin et al., 2012a) likely reflects improved resolution of mesoscale meteorology at higher resolution and the damping of vertical eddy transport at coarser resolution (Wang et al., 2004; Zhang et al., 2011).

AM3 simulates a wider NAB range than GEOS-Chem (Figure 6 and Table 3). This wider range of NAB may contribute to the wider total surface O₃ distribution in the AM3 versus GEOS-Chem standard simulations, which aligns more closely with the observed variability, except for O₃ simulated with the high-resolution GEOS-Chem model in summer at high-altitude sites. The relative skill of AM3 in capturing the variability of NAB despite its generally high bias implies that AM3 is useful for process-level analysis and for quantifying day-to-day variability. We underscore the need for future efforts to focus on specific processes and describe below (Section 3.4) some first steps towards this goal.

In Table 3, we further partition statistics for total and NAB O₃ in surface air into average versus high-O₃ days. We use observed values, rather than simulated values used in Zhang et al. (2011), to select for high-O₃ days in order to sample the same temporal subset from both models. Using the simulated total O₃ values would lead to subsets of different sizes given the individual model biases. During spring, the models robustly estimate NAB to be ~10 ppb higher on average at high-altitude than at low-altitude CASTNet sites, but AM3 estimates higher NAB levels than GEOS-Chem. During summer, the models also estimate higher NAB at high-altitude than at low-altitude sites, and average NAB levels decrease from spring to summer at low-elevation sites. GEOS-Chem suggests little change from spring to summer in average high-altitude NAB whereas AM3 simulates a decrease of over 10 ppb. At the high-altitude sites, both models suggest that NAB increases as total O₃ increases, although the sample size is small for events above 75 ppb and the average values for the different data subsets all fall within one standard deviation each other. At the low altitude sites, there is little change in the average NAB when selecting for observed values exceeding 60, 70, or 75 ppb. The

variability in NAB, as measured by the standard deviation in Table 3, is similar in the two models at the low-elevation sites, but AM3 simulates more variability in NAB at the high-altitude sites than GEOS-Chem, particularly on high-O₃ days.

The time series in Figure 7 provide evidence at the local scale for our assessment of regional and seasonal biases. At the two western U.S sites (Gothic, CO and Grand Canyon NP, AZ) in Figure 7, the 6-month average NAB is nearly the same in both models, but this reflects little seasonal variation in the GC NAB (thin blue line) versus a sharp seasonal decline from spring into summer in AM3 (thin red line). The standard deviation is twice as large in AM3 as in GEOS-Chem, consistent with the frequency distributions of NAB in Figure 6 (left side) and with the observed variability.

We further probe the time series in Figure 7 by calculating correlation statistics separately for the spring and summer seasons (Table 4). During spring, the correlations at the WUS sites are higher in GEOS-Chem (Table 4), but AM3 maintains the same level of correlation into summer at the Colorado site while the correlation improves into summer at the Arizona site. Table 4 also shows the correlation of the NAB estimates versus the simulated total O₃. Over the WUS sites, the models robustly indicate that variability in NAB drives a substantial portion of the total surface O₃ variability in both seasons, but with a stronger influence (higher correlations) during spring.

Despite the summertime high bias in AM3 at the two EUS sites (M.K. Goddard, PA and Georgia Station, GA), it correlates at least as well with the observations as GEOS-Chem (Figure 7, Table 4). At the EUS sites in Figure 7, the NAB in both models is poorly correlated, and in some cases, anti-correlated with the total simulated surface O₃. An important implication is that the highest total surface O₃ events are generally decoupled from the highest NAB events, consistent with the current understanding that regional pollution is the dominant influence on total O₃ distributions in this region.

3.4 Processes contributing to inter-model differences in total and NAB surface O₃

We examine here the role of specific processes in contributing to differences in the GEOS-Chem and AM3 Base and NAB simulations. Superimposed in Figure 7 are results from a separate simulation (Lin et al., 2013) in which a stratospheric O₃ tracer (O3Se90) was available, tagged relative to the e90 tropopause (Prather et al., 2011) as

described in Lin et al. (2012a). The correlation of the O3Se90 tracer with the NAB in AM3 is also provided in Table 4. The high summertime correlation of O3Se90 and NAB at the WUS sites (Figure 7) does not imply that stratospheric O₃ intrusions are the dominant factor as the magnitude of the O3Se90 enhancements in summer can not explain the full magnitude of the episodic NAB enhancements. Rather, this result implies that other sources enhance NAB free tropospheric O₃, which then mixes into the surface air alongside the O3Se90 tracer in the model. We interpret the high correlations in both seasons at the EUS sites (Figure 7) in a similar manner: the O3Se90 indicates a larger influence of O₃ mixing down from the free troposphere.

3.4.1 Deep stratospheric intrusions over the WUS in spring

As described in Lin et al. (2012a), stratospheric O₃ drives a substantial portion of the daily variability in observed springtime O₃ over the Western U.S. Inspection of Figure 7 (top two panels) shows that the episodic enhancements in the O3Se90 tracer can explain much of the episodic enhancements in NAB. A caveat is that the magnitude of the stratospheric contribution is an upper limit due to the definition of the O3Se90 tracer, which could be tagging O₃ in the lower stratosphere that originated in the troposphere (estimated to be approximately half of the O3Se90 during spring by Zhang et al., 2013). Nevertheless, the strong correlation of the orange and red lines in Figure 7 implies a key role for transport and mixing of free tropospheric air into the planetary boundary layer in driving day-to-day variability in NAB O₃ levels.

For illustrative purposes, we focus on an event during late May of 2006 at the Gothic and Grand Canyon sites, during which the AM3 model NAB (thin red line in Figure 7) spikes, with an associated increase in the simulated total O₃ (thick red line). In contrast, GEOS-Chem NAB (thin blue line) decreases, as does total O₃ (thick red line) during this event. The opposing trends in the models during this event raise questions as to whether both models simulate a mixing event but import different NAB levels, or whether the boundary layer in AM3 mixes more vigorously with the free troposphere than in GEOS-Chem. The observations (black) increase during this period, as captured by AM3 over the model overestimates the observed values on May 27 and 28.

Figure 8 shows spatial features in OMI total O₃ columns and in OMI/MLS tropospheric O₃ columns that are characteristic of stratospheric intrusion events, as previously documented during the spring of 2010 by Lin et al. (2012a). Both models indicate enhanced NAB at 500 hPa in the location where the satellite columns are enhanced, but the magnitude is much higher in AM3 (Figure 8), consistent with the higher surface NAB over this region (left column of Figure 9). Comparison with O₃ measured at the ground-based CASTNet sites during this period shows that AM3 captures the observed pattern of enhancements over the Four Corners region, but overestimates the magnitude (Figure 9). While the OMI/MLS tropospheric O₃ product demonstrates that stratospheric O₃ did penetrate into the troposphere (Figure 8), it is inconclusive as to whether it mixed down into the planetary boundary layer. The O3Se90 tracer (orange line in Figure 7) suggests that the AM3 model is simulating surface O₃ enhancements associated with a stratospheric intrusion and consistent with the observed spatial pattern of enhanced ground-level O₃ at the CASTNet sites. Figure 7 and Table 4 further suggest that these events drive much of the variability in NAB at high-altitude western sites in spring (Figure 7 and Table 4), consistent with earlier findings for April through June of 2010 (Lin et al., 2012a).

3.4.2 Wildfires over the EUS in spring and summer

There are several EUS events during spring and summer where AM3 simulates a localized spike in NAB that is not simulated by GEOS-Chem, which we attribute at least partially to the differing treatment of wildfire emissions in the models. In AM3, the recommendations from Dentener et al. (2006) are applied to vertically distribute biomass burning emissions, placing 40% of the total emissions between 3 and 6 km (see their Table 4) over boreal North America. In AM3, this recommendation was applied north of 25°N and likely contributes to the summertime O₃ overestimates at 500 hPa over Canada (Figure 4). Vertical mixing of NAB O₃ from the free troposphere into surface air in the AM3 model is indicated by associated enhancements of the O3Se90 tracer on days with high NAB. In contrast, biomass burning is emitted only in the boundary layer in GEOS-Chem, likely resulting in less efficient O₃ production and subsequent long-range transport. The GEOS-Chem approach appears more consistent with the observations.

We illustrate this point in more detail by analyzing an extreme “NAB event” in the AM3 model on June 28, 2006 at the Pennsylvania CASTNet site in Figure 7 (bottom panel). AM3 estimates NAB values above 60 ppb, exceeding the total observed value of about 60 ppb, while GEOS-Chem simulates NAB below 20 ppb (Figure 7, yellow highlight). The AM3 event is attributed at least partially to transport of boreal biomass burning emissions, based on back-trajectory analysis from NOAA’s HYSPLIT model for June 28, 2006 (Figure 10), driven with the same NCEP wind fields to which AM3 was nudged. The back-trajectory indicates that the free tropospheric air mass associated with the event passed over Canadian fires. The lofting of fire effluents in the model likely produced PAN that was transported in the free troposphere from Canada to the U.S., subsided, and thermally decomposed into NO_x, leading to O₃ production. This interpretation is consistent with the enhanced PAN and NAB O₃ concentrations at 750 hPa collocated with the late June event (Figure 10) and others like it in the AM3 model. In addition to the differences in vertical distribution of fire effluents, GEOS-Chem uses a fire emission inventory specific to the year 2006 whereas AM3 applies a climatological inventory (Table 2). We find that the use of a year-specific fire inventory versus a climatology in AM3 leads to differences of 10 ppb for the June 28, 2006 event (not shown).

3.4.3 Lightning NO_x over the Southwestern United States in summer

GEOS-Chem produces approximately 10 times more lightning NO_x than AM3 over the southwestern U.S. during summer (0.018 Tg N in AM3 versus 0.159 Tg N in GC within the region 26°N-42°N, 124°W-97°W) and the models further differ in their spatial distributions of the lightning NO_x source (Table 2). The models differ markedly in their NAB estimates over this region in summer (e.g., Figures 1 and 2). This source has been reduced in a newer version of GEOS-Chem, decreasing simulated NAB O₃ in these regions (Zhang et al., 2013).

During August at the two WUS sites in Figure 7, the models reverse their relative rankings of simulated NAB relative to springtime, with the GEOS-Chem NAB as much as 10-20 ppb higher than AM3 NAB in summer. In notable contrast to the spring, GEOS-Chem overestimates the observed O₃ values. We attribute the summertime

overestimate and poor correlations of GEOS-Chem with the observed values over the two WUS sites in Figure 7 (Table 4) to the lightning NO_x source and subsequent transport.

3.4.4 Isoprene oxidation chemistry over the EUS in summer

Earlier work (*e.g.* Fiore et al. 2002, 2003) demonstrated that NAB is fundamentally different between the EUS and the WUS, with the EUS more strongly controlled by regional photochemistry, where the O_3 lifetime in the planetary boundary layer is as short as 1-2 days and isoprene- NO_x - O_3 chemistry dominates much of the region from May through September (Jacob et al., 1995). At the two EUS sites in Figure 7 (M.K. Goddard, PA and Georgia Station, GA), we attribute some of the differences in the summertime simulations to the isoprene oxidation mechanism (Table 2) that would tend to reduce O_3 production in GEOS-Chem relative to AM3 due to isoprene ozonolysis serving as a more important loss pathway for NAB in GEOS-Chem (Fiore et al., 2002; Mickley et al., 2001). These differences in isoprene oxidation chemistry could at least partially explain the higher NAB in AM3 during the isoprene emission season (*i.e.*, a longer O_3 lifetime in the AM3 boundary layer). The largest inter-model differences in NAB, however, occur in spring when transported sources are more important than regional production involving natural sources.

The isoprene oxidation chemistry likely also contributes to the large bias in AM3 total surface O_3 . GEOS-Chem assumes a much higher yield of isoprene nitrates from the reaction of isoprene hydroxyperoxy radicals with NO and assumes they are a permanent sink of NO_x (Table 2). In contrast, AM3 assumes an 8% isoprene nitrate yield and allows 40% of the products to recycle back to NO_x on the basis of observational constraints from field campaigns (Horowitz et al., 2007; Perring et al., 2009). Earlier work with predecessors of the models used here suggests that these differences may explain over 10 ppbv of the high bias in AM3 relative to GEOS-Chem over the EUS in summer (Fiore et al., 2005). The fact that GEOS-Chem best captures the observations implies that the additional O_3 production from isoprene oxidation using the field-based constraints on isoprene nitrates must be offset by larger O_3 losses, such as from additional HO_x uptake by aerosol (Mao et al., 2013) and halogen-induced O_3 destruction (Parrella et al., 2012).

4. Inter-annual variability in NAB MDA8 O₃ estimates in surface air

The 27-year AM3 NAB simulation (1981-2007) enables us to define spring and summer climatologies of seasonal mean NAB O₃ in surface air, and to quantify the year-to-year variability as the standard deviation of the annual seasonal mean values (Figure 11). The seasonal mean spatial patterns are similar to those in 2006 (Figure 1), with little year-to-year variation over much of the country. Figure 11 also includes the climatological fourth highest MDA8 value between March 1 and August 31 over the multi-decadal simulation. We emphasize that these estimates are subject to the biases diagnosed above in comparison to observations. In particular, NAB estimates over the EUS are probably too high in AM3. The variability over central Texas and central Mexico in the fourth highest values may indicate year-to-year variations in events involving NAB production from lightning NO_x and convective mixing. Large variability in both mean NAB levels and the highest events is simulated over Western Colorado in spring, with standard deviations of 2-3 ppb, likely reflecting variability in year-to-year influence from stratospheric O₃ intrusions.

Jaffe (2011) noted regionally coherent year-to-year variability in the number of high-O₃ events at high-altitude western U.S. measurement sites in both spring and summer and we examine here the potential contribution of NAB to this observed variability. Specifically, Jaffe (2011; see their Figure 6) found that the number of O₃ events above thresholds of 65, 70, and 75 ppb varied together, with the lowest and highest number of springtime events occurring in 1997 and 1999, respectively; for summer, the lowest and highest years were 1997 and 2002. We follow the approach of Wang et al. (2009; see their Figure 5) to illustrate simultaneously the model skill at capturing the observed values, and the simulated NAB contribution to observed levels within specific ranges for total surface O₃. Figure 12 shows the AM3 NAB contributions throughout the overall observed distributions for 2006 in comparison to a low versus high year for observed high-O₃ events at the same 12 intermountain West sites used by Zhang et al. (2011), permitting a direct comparison with the GEOS-Chem estimates in their Figure 3. Note that the highest years differ for spring and summer, but the lowest year is 1997 in both seasons.

For observed O₃ events above 60 ppb, AM3 tends to overestimate observations during spring but does not exhibit any systematic bias during summer. Furthermore, the model captures events up to 80 ppb during spring of 1999, though in other years there is a general tendency to underestimate events above 75 ppb. This finding contrasts with those from higher-resolution models including the GEOS-Chem version used here, which underestimates events above 60 ppb (Zhang et al., 2011). During all years and both seasons shown in Figure 12, there is a tendency for the median simulated NAB contribution to increase from observed values of 40 ppb to those in the 70 ppb range, with 75th percentile values reaching 50-60 ppb for observed values above 60 ppb during 2006 and 1999, implying that enhanced NAB levels contribute to the higher observed values. This interpretation is consistent with the findings of Lin et al. (2012a) that stratospheric O₃ intrusions over the high-altitude western U.S. drive much of the observed day-to-day variability in spring, as well as with Jaffe (2011) who suggests that a large-scale process drives coherent variability at the monitoring sites in this region.

Consistent with earlier work (Fiore et al., 2003), Figure 12 shows that summertime NAB levels are typically much lower than in spring, with maximum values nearly always below 60 ppb and 75th percentile values generally below 50 ppb. Jaffe (2011) suggested that summertime inter-annual variability is strongly influenced by wildfire activity. The lack of year-to-year variations wildfires in this version of the AM3 model may contribute to its underestimate of the highest events in 2002 and 2006, which were the first and second highest fire activity years for the 1997-2006 period analyzed by Jaffe (2011).

5. Conclusions and Recommendations

On the basis of health evidence, the threshold for the National Ambient Air Quality Standard for ground-level O₃ has been lowered in recent years, pushing closer to “background” levels. In the past, the U.S. Environmental Protection Agency considered model-based estimates of background O₃ as part of the process for setting the NAAQS. These model-based estimates, previously called “Policy-Relevant Background”, are now termed “North American Background” (NAB), which is defined to be background levels that would exist in the absence of North American anthropogenic emissions. Identifying

high-background events is crucial for determining whether an observation merits consideration for “exceptional event” status, which exempts a particular observation from counting towards non-attainment if it can be shown that the event occurred due to processes beyond the control of U.S. air quality management options. The model simulations presented here can provide information on the frequency of such events and the individual components contributing to NAB, including O₃ originating from international pollution, wildfires, or the stratosphere.

As a first step towards assessing our understanding of NAB and its components, we briefly reviewed recent model estimates (Table 1). We then evaluated total surface O₃ and NAB estimates from two independent models (GEOS-Chem and AM3) for March through August of 2006, using comparisons between the base simulations and space-based and ground-based measurements to place constraints on the model estimates. A 27-year NAB simulation in the AM3 model provides context for our two-model analysis and indicates that 2006 is a typical year in terms of its spatial and seasonal patterns in NAB, though 2006 NAB levels are generally higher than the climatological averages (compare Figure 11 with 1 and 2). The largest variability in mean NAB MDA8 estimated with AM3 occurs over Idaho, western Colorado and Wyoming, and New Mexico, with standard deviations of over 2 ppb; the largest variability in the fourth highest MDA8 NAB occurs over Colorado and Texas (Figure 11). A comparison of low- versus high-O₃ years at high-altitude WUS sites indicates a role for NAB in driving year-to-year differences in the frequency of springtime high-O₃ events (Figure 12).

At high-altitude WUS sites, the GEOS-Chem and AM3 models consistently show higher NAB than at low-altitude sites, but the magnitude and day-to-day variability often differs (Figures 1,5,6,7, Tables 3,4). In some months (*e.g.*, August), the larger differences between the NAB estimates from the two models than between the simulated and observed total O₃, imply that agreement with observations, while a necessary condition, does not sufficiently constrain the NAB estimates. While AM3 indicates a seasonal decline of NAB into summer over this region, GEOS-Chem suggests a relatively weak seasonal cycle associated with an increase of influence from lightning NO_x in that model during the late summer (Figures 5 and 7). Higher stratosphere-troposphere exchange in AM3 may explain the springtime NAB enhancement in the free troposphere

relative to GEOS-Chem (Figure 3), which, followed by more vigorous mixing between the free troposphere and boundary layer, may explain the higher NAB in surface air during this season in AM3 (Figure 1).

At low-altitude sites, such as over the EUS, the models consistently show lower NAB levels than at high-altitude sites, as in earlier work (Table 1). We find that the highest total surface O₃ events over the EUS are often decoupled from the highest NAB events, consistent with the understanding that regional pollution is the dominant influence on total O₃ distributions there. Over the EUS, uncertainties in isoprene-NO_x-O₃ chemistry (Table 2) likely contribute to differences in simulated total O₃, and to a lesser extent, NAB estimates.

We find little evidence that horizontal resolution is a major contributor to differences in mean NAB estimates in the models (Figure 6), consistent with EPA (2013). Higher resolution refines spatially local NAB estimates, including at the tails of the distribution and is also important for resolving the impact from local and regional emissions, as evidenced by the larger differences associated with resolution in summertime distributions when photochemical production peaks in many U.S. regions (Figure 6). We conclude that simulated NAB distributions reflect large-scale synoptic transport that is resolved sufficiently at the relatively coarse scale of global models, with the NAB differences mainly stemming from different treatments of NAB sources such as stratospheric O₃, boreal fires, and lightning NO_x. The regional and seasonal variability in these driving processes further manifests as differences in the model timings of the fourth highest NAB over many regions (Figure 2).

Future efforts to determine the processes contributing to model differences, and to the biases in individual models versus observations, would benefit from evaluation with daily ozone vertical profiles as measured by sondes, consistently defined tracers of stratospheric influence (e.g., the O3Se90 tracer in AM3), as well as daily three-dimensional archival of other chemical species (e.g., CO, PAN, H₂O) that can aid in disentangling tropospheric versus stratospheric origins and from meteorological variables (e.g., mixing depth, mass fluxes) to diagnose the role of mixing processes. The routine use of synthetic tracers could further aid in distinguishing between model differences in transport, dilution, and mixing versus chemical evolution during transport. Improved

estimates of NAB in a given region and season will require better constraints on, for example: lightning NO_x for central and Southwestern U.S. in summer; transported stratospheric O₃ over the high-altitude Western U.S. in spring; isoprene chemistry and its impact on chemical processing and NAB lifetime over the EUS in summer; and wildfires which may influence NAB throughout the nation from late spring into summer.

We propose that future multi-model studies target limited time periods to enable process-oriented analysis during field campaigns when ground-based and satellite observations are supplemented with a broader suite of observations from intensive aircraft flights and balloon launches. If combined with a thorough evaluation of O₃ precursors, such analysis should hasten progress towards understanding the impact of specific sources on NAB O₃. We further recommend developing bias-correction techniques, such as those routinely applied in numerical weather prediction, to improve the accuracy of local NAB estimates. As a first step, simple assumptions assuming the bias is entirely driven by one process (*e.g.*, as applied to the stratospheric O₃ estimates from the AM3 model by Lin et al. (2012a)) can be applied to individual models and then used to generate a multi-model estimate with uncertainties. The two models analyzed here often bracket the observations (Figures 3-7, and 9), thereby indicating different sources of error, which leads us to conclude that a multi-model approach can harness unique capabilities of different modeling systems and thus provide more accurate NAB estimates than a single model.

Acknowledgments. We acknowledge support from the NASA Air Quality Applied Sciences Team (NNX12AF15G to AMF; NNX11AH93G to DJJ), the NOAA Ernest F. Hollings Scholarship program (JTO) and NOAA GFDL. We are grateful to P. Dolwick (U.S. EPA) for useful discussions and comments. The information in this article has been subjected to review by the National Center for Environmental Assessment, U.S. Environmental Protection Agency, and approved for publication. Approval does not signify that the contents reflect the views of the Agency.

Table 1. Model estimates for North American Background (NAB) ozone using current U.S. EPA definition (North American anthropogenic emissions set to zero) and for specific components of NAB (ppb)

Study Model	Study period; Metric	NAB	Components
Fiore et al. (2003) GC (2°x2.5°)	Mar-Oct 2001; 1-5pm mean	Typically 15-35; up to 40-50 (highest in spring an WUS)	<i>Natural</i> : 18-23 (NW), 18-27 (SW), 13-20 (NE), 15-21 (SE) <i>Strat</i> : always < 10 <i>CH4+ICT</i> : 5-12
Wu et al. (2008) ; GC with winds from GISS GCM (4°x5°)	2000 clim.; 1-5pm mean	12-30 (summer); 22-40 (April); highest in WUS	<i>Natural</i> : 10-15 (EUS, summer); 15-25 (WUS, summer)
Wang et al. (2009) GC (1°x1°)	summer 2001; MDA8	26±8 <i>USB</i> : 30±8; up to 33 ppb during events	
Zhang et al. (2011) GC (1/2°x2/3°)	Mar-Aug 2006- 2008; MDA8	39-44 (spring); 35- 45(summer); low-alt 27±8; high-alt 40±7; 51-59 (4 th highest)	<i>Natural</i> : 18±6 (low-alt); 27±6 (high-alt); 34-45 (4 th highest). <i>CH4+ICT</i> : 13-16 (spring) 11-13 (summer); 13 (high alt); 9 (low alt)
Emery et al. (2012) CAMx (12 km ²), GC BCs	Mar-Aug 2006; MDA8	25-50 ppb (20-45 in GC); 35-100 (4 th highest; 65 max without fires; 55 max in GC)	<i>Fires</i> : 10-50 ppb (events)
Lin et al. (2012a) GFDL AM3 (~50km ²)	Apr-Jun 2010; MDA8	15 WUS high-alt sites: 50±11 (mean); 55±11 (days when obs exceed 60 ppb)	<i>Strat</i> : 15 WUS high-alt sites: 22±12 (mean); 15-25 for obs O ₃ @ 60-70; 17-40 for obs O ₃ @ 70-85 <i>Median, bias-corrected</i> : 10-22 (W); 8-13(NE); 3-8 (SE) <i>Max, bias-corrected</i> : 35-55 (W); 30-45 (EUS)
McKeen et al. (2002); 3D regional model (60 km ²)	Jun-Jul 1995; 1-4pm mean		<i>Fires</i> : 10-30 ppb (event, Central and EUS)
Collins et al. (2003);	March 1991		<i>Strat</i> : 5-15 ppb (highest in WUS)

STOCHEM driven by UM HadAM4 GCM)	1994 monthly mean		
Kaynak et al. (2008); CMAQ (36km ²)	Jul-Aug 2004; MDA8		<i>Lightning</i> : up to 10 ppb; 14 ppb 4th highest; < 2 ppb 71% of the time
Mueller and Mallard (2011); CMAQ, GC BCs (36 km ²)	2002; MDA8		<i>Fires</i> : 30-50 (WUS, events) <i>Lightning</i> : 10-30 (Southern US, events)

Table 2. GFDL AM3 and GEOS-Chem model configurations

Model	GFDL AM3 Donner et al. (2011) Rasmussen et al. (2012) Naik et al. (2013) Lin et al. (2012b)	GEOS-Chem http://acmg.seas.harvard.edu/geos/ (Zhang et al., 2011) (Bey et al., 2001) (Park et al., 2004)
Grid	Cubed sphere with 48x48 cell faces, approximately 2°x2° horizontal resolution. Vertical coordinate is a 48-level hybrid sigma grid, with the top level at 0.01 hPa; lowest 5 layers extend to 60, 130, 220, 330, and 470 m for surface pressure of 1013.25 hPa and scale height of 7.5km.	Continental North American nested (Wang et al., 2004) simulation at ½° latitude by ⅔° longitude using boundary conditions from boundary conditions from a 2°x2.5° global simulation. Vertical grid has 47 levels to 0.01 hPa, with lowest 5 layers centered at 70, 200, 330, 470, 600 m for a column at sea level.
Meteorology	Online, nudged to NCEP <i>u</i> and <i>v</i> (Kalnay et al., 1996). The nudging timescale is inversely proportional to pressure (Lin et al., 2012b)	Assimilated from NASA GEOS-5
Stratospheric ozone	Stratospheric chemistry and dynamics seamlessly coupled to the troposphere (Naik et al., 2013)	Linoz parameterization (McLinden et al., 2000)
Isoprene nitrate yield and fate	Observationally-constrained 8% yield with 40% NO _x recycling (Horowitz et al., 2007 and references therein)	18% yield with no NO _x recycling (permanent sink for NO _x)
Lightning NO _x distribution	Parameterized based on convective cloud top height (Price and Rind, 1992), and described in Horowitz et al. (2003); source in 2006 is 4.9 Tg N a ⁻¹ ; range over 1981-2007 is 4.4-4.9 Tg N a ⁻¹ .	Scaled to match a top-down constraint of 6 Tg N a ⁻¹ (Martin et al., 2007) and spatially redistributed based on the LIS/OTD flash climatology (Murray et al., 2012) and includes a higher yield (500 mol N flash ⁻¹ at northern mid-latitudes and 125 mol N flash ⁻¹ elsewhere (Hudman et al., 2007)
Anthropogenic emissions	ACCMIP (Lamarque et al., 2010) with annual interpolation after 2000 to RCP4.5 2010 value (Lamarque et al., 2011)	EDGAR (Olivier and Berdowski, 2001) with U.S. emissions from 2005 National Emissions Inventory (NEI-05)

Biogenic emissions	Model of Emissions of Gases and Aerosols from Nature (MEGAN) 2.1 (Guenther et al., 2006), implemented as described by Emmons et al. (2010) and Rasmussen et al. (2012)	MEGAN 2.0 (Guenther et al., 2006)
Biomass burning emissions	As for anthropogenic emissions but distributed vertically as recommended for AeroCom (Dentener et al., 2006)	GFEDv2 year-specific monthly fires (van der Werf et al., 2006), emitted at surface

Table 3. Summary statistics of seasonal mean MDA8 total and NAB O₃ in surface air (ppb) as observed and estimated with the GFDL AM3 and GEOS-Chem (GC) models, segregated by altitude, season, and observed values.

Season	Filter	N	OBS	AM3 Base	GC Base	AM3 NAB	GC NAB
<i>Above 1.5 km (excluding CA)</i>							
MAM	None	993	57±7	60±7	54±6	48±8	42±5
MAM	Obs ≥ 60	300	64±4	63±7	58±6	52±8	45±5
MAM	Obs ≥ 70	33	73±4	66±6	62±4	55±7	47±5
MAM	Obs ≥ 75	7	80±4	65±7	61±2	56±8	50±3
JJA	None	899	58±7	55±6	57±8	35±8	40±7
JJA	Obs ≥ 60	344	65±4	58±5	59±7	38±8	41±6
JJA	Obs ≥ 70	38	73±5	61±4	62±7	43±8	42±6
JJA	Obs ≥ 75	9	80±6	64±4	64±6	47±6	42±3
<i>Below 1.5 km</i>							
MAM	None	5769	49±11	57±8	48±8	39±8	29±7
MAM	Obs ≥ 60	969	65±6	64±8	57±8	37±8	29±7
MAM	Obs ≥ 70	175	75±6	69±8	63±10	36±10	31±8
MAM	Obs ≥ 75	58	82±6	71±10	68±12	36±11	34±9
JJA	None	5583	51±15	69±15	54±14	29±9	24±8
JJA	Obs ≥ 60	1509	69±9	76±13	63±11	30±9	25±9
JJA	Obs ≥ 70	537	78±8	77±13	67±12	30±9	27±10
JJA	Obs ≥ 75	294	83±8	76±14	69±14	31±9	28±10

Table 4. Correlation coefficient (r) by season for the time series in Figure 7.

	Gothic NP, CO		Grand Canyon NP, AZ		Georgia Station, GA		M.K.Goddard, PA	
	MAM	JJA	MAM	JJA	MAM	JJA	MAM	JJA
AM3 vs. OBS	0.5	0.51	0.41	0.66	0.55	0.63	0.74	0.65
GC vs. OBS	0.56	-0.08	0.62	0.29	0.69	0.48	0.69	0.62
AM3 NAB vs. total	0.87	0.62	0.87	0.64	-0.41	0.25	-0.29	-0.37
GC NAB vs. total	0.81	0.73	0.61	0.48	0.06	0.15	0.15	-0.05
AM3 O3Se90 vs. NAB	0.85	0.87	0.88	0.9	0.87	0.9	0.93	0.91

Figures.

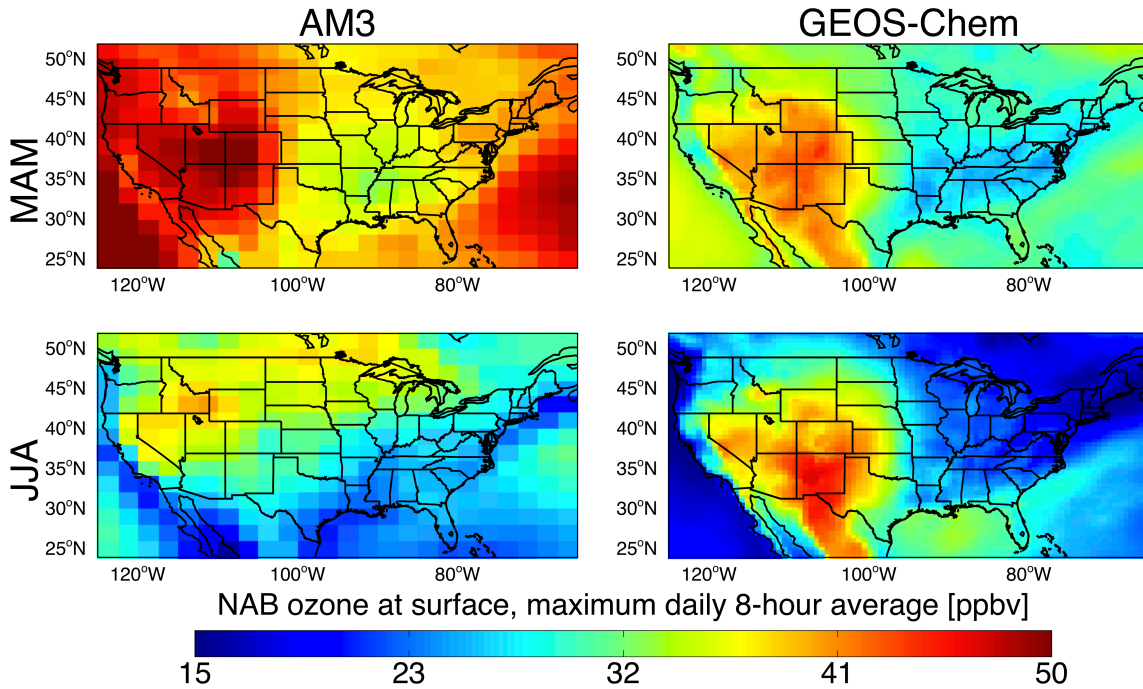


Figure 1. Mean MDA8 values of North American Background (NAB) in the lowest model layer for the GFDL AM3 (left; $\sim 2^\circ \times 2^\circ$ horizontal resolution) and GEOS-Chem (right; $\frac{1}{2}^\circ \times \frac{2}{3}^\circ$) simulations for spring (MAM; top row) and summer (JJA; bottom row) of 2006. NAB is estimated with simulations in which North American anthropogenic emissions are set to zero. See Table 1 for model configurations.

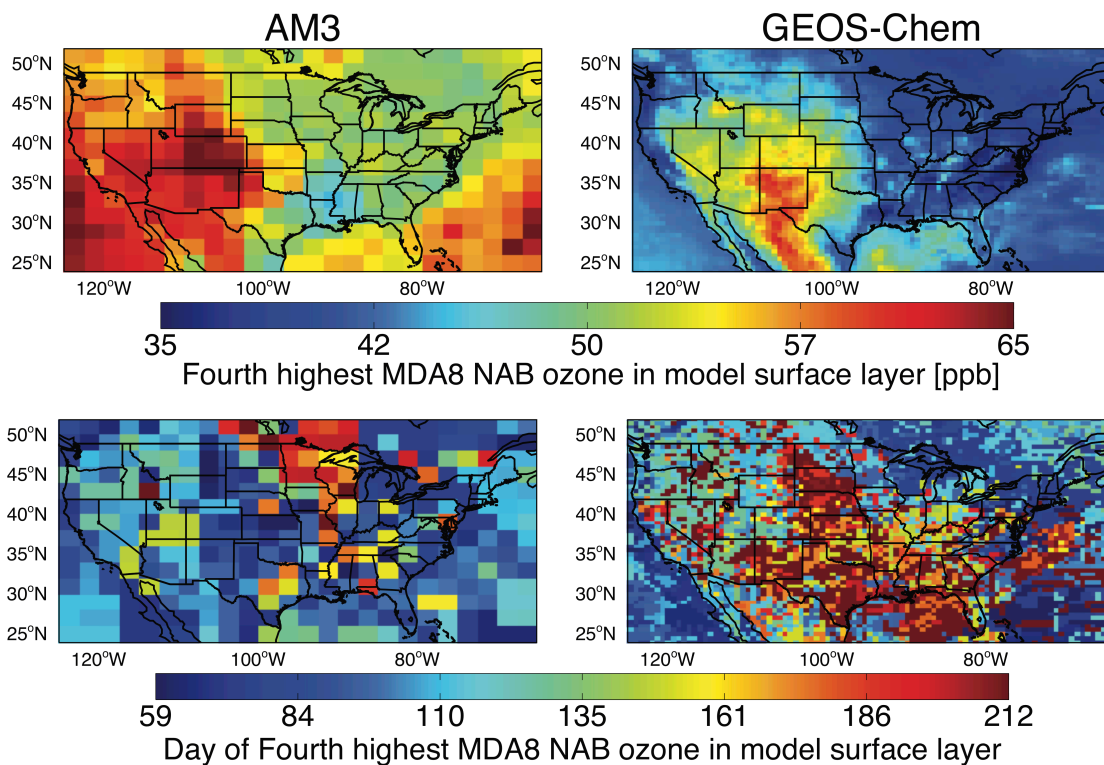


Figure 2. Fourth highest MDA8 NAB O₃ between March 1 and August 31 2006 in the lowest model layer (top) and date of occurrence (bottom) for GFDL AM3 (left; $\sim 2^\circ \times 2^\circ$ horizontal resolution) and GEOS-Chem (right; $\frac{1}{2}^\circ \times \frac{2}{3}^\circ$) simulations.

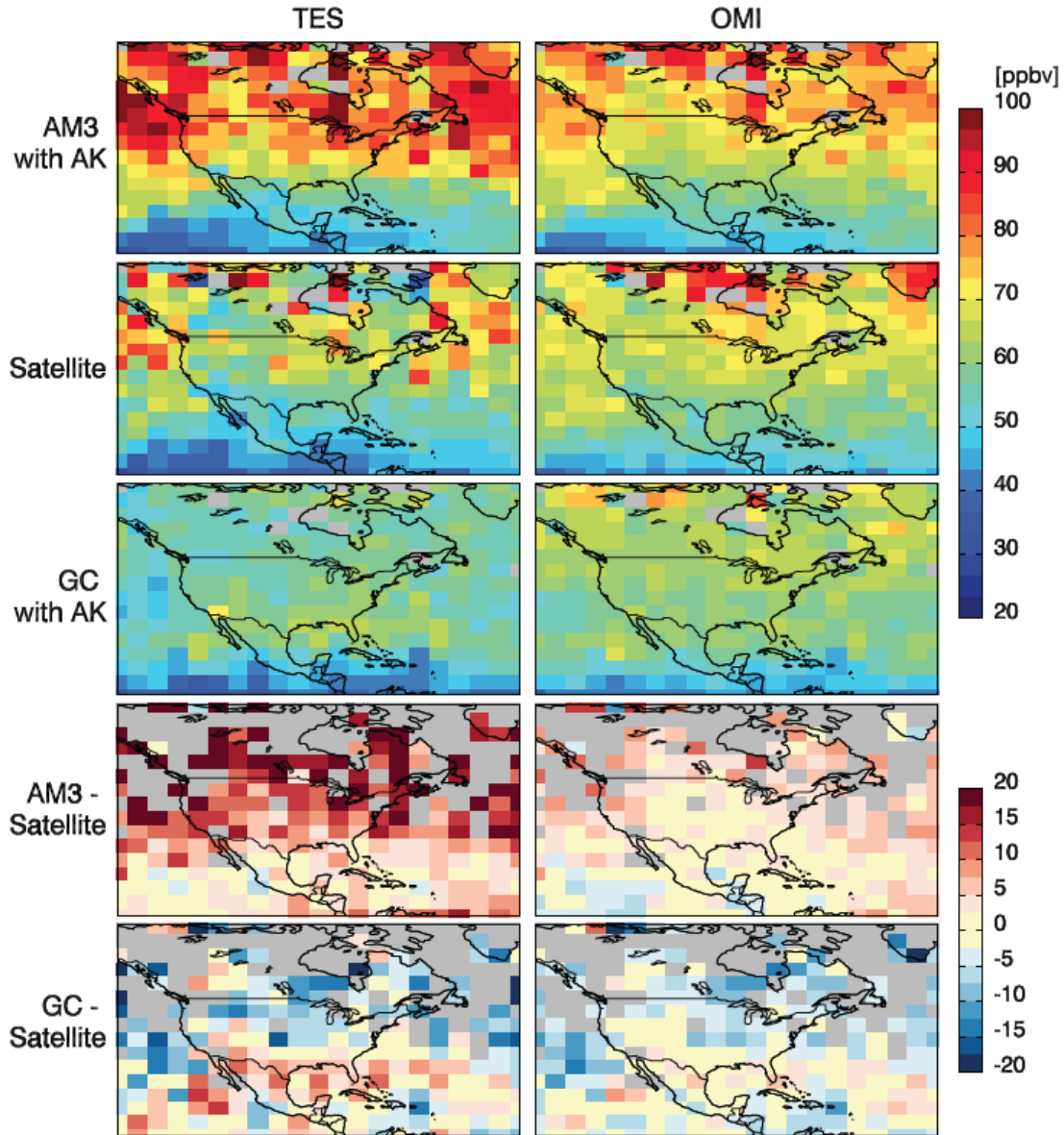


Figure 3. Springtime (March-April-May average) mid-tropospheric O₃ as retrieved (second row) from the TES (left column) and OMI (right column) satellite instruments and as simulated with the GFDL AM3 (top row) and GEOS-Chem (third row) with the appropriate averaging kernels applied to daily average O₃ fields archived from the models. Grey boxes denote locations where no coincident TES and OMI data points meet the retrieval quality criteria. The simulations evaluated here are at coarse horizontal resolution ($\sim 2^\circ \times 2^\circ$) in both models, after removing the 2005-2007 annual average bias of the satellite products (5.7 ppb for TES; 3.1 ppb for OMI) relative to ozone sondes between 20-60°N determined by Zhang et al. (2010). The third and fourth rows show the difference of the simulated mid-tropospheric O₃ with each satellite product; grey boxes denote places where the OMI and TES retrievals disagree by over 10 ppb.

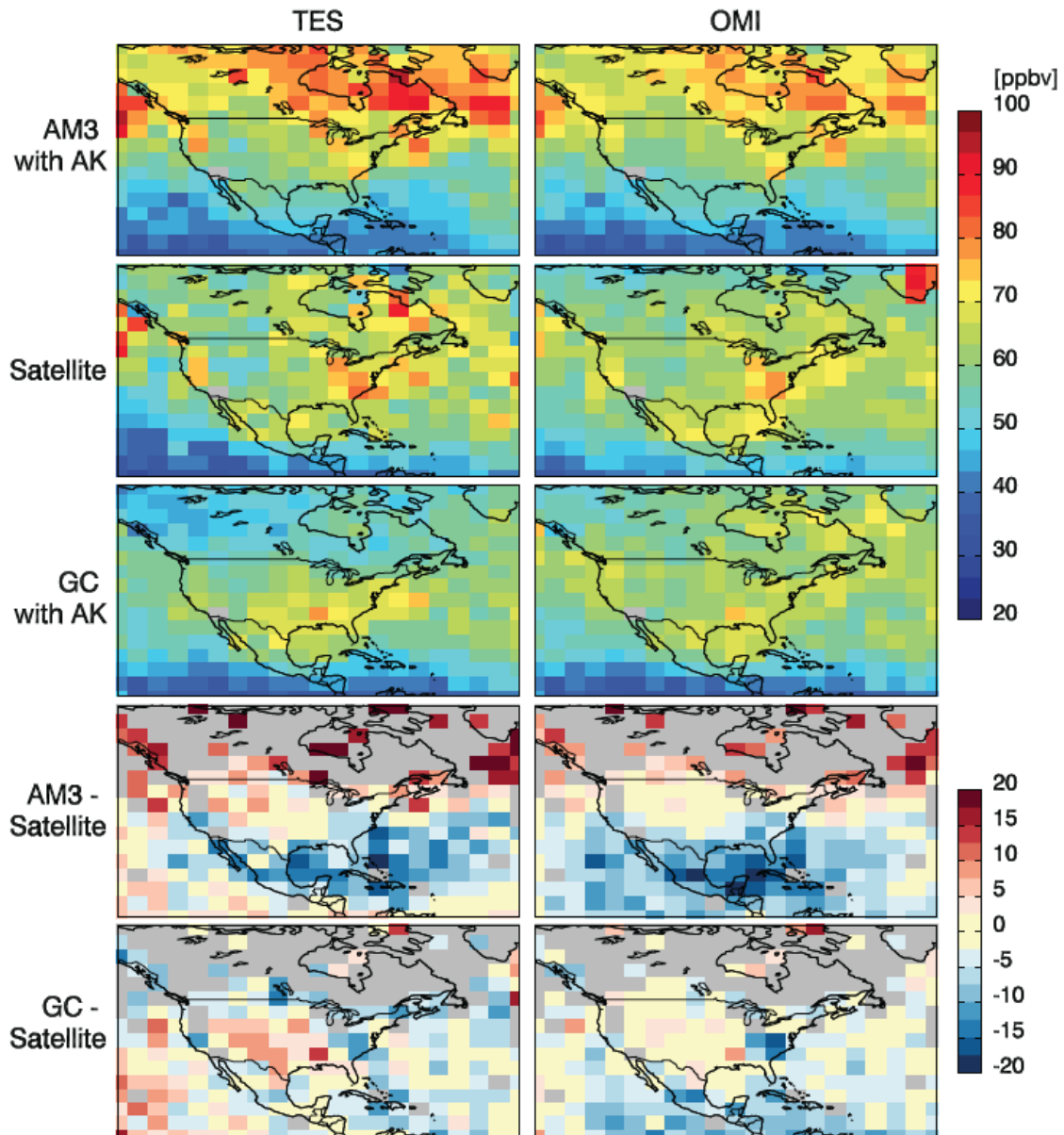


Figure 4. As in Figure 3 but for summer (June-July-August).

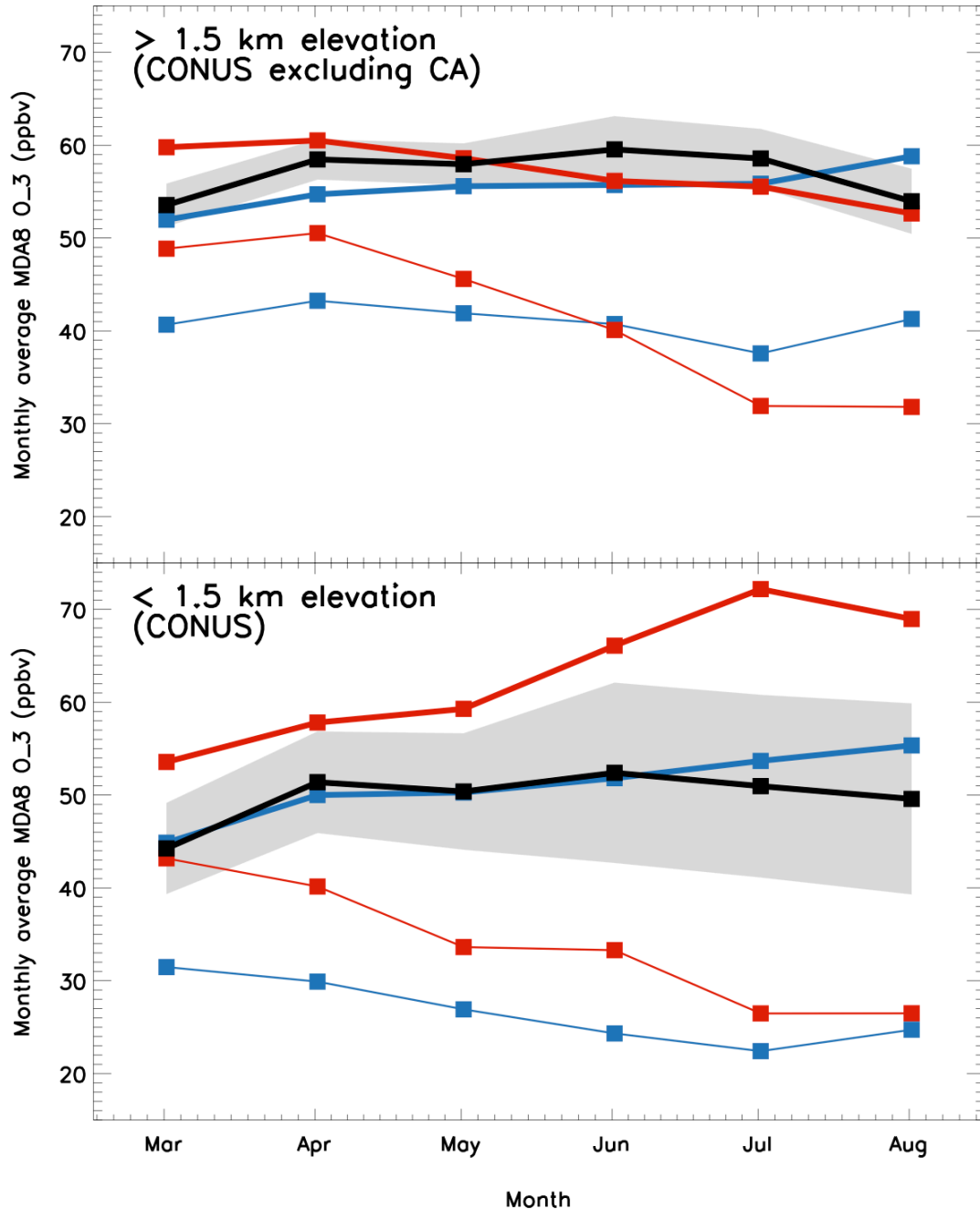


Figure 5. Monthly mean MDA8 values for March through August of 2006 in CASTNet observations (black) and the standard simulations (thick lines) for the GEOS-Chem ($GC \frac{1}{2}^{\circ} \times \frac{2}{3}^{\circ}$ horizontal resolution; blue) and GFDL AM3 ($\sim 2^{\circ} \times 2^{\circ}$ horizontal resolution red) simulations sampled at the CASTNet sites (using bilinear interpolation of the nearest four grid cells and sampling only on days with valid measurements) at altitudes a) above 1.5km excluding California to focus on the InterMountain West region and b) below 1.5km in altitude. Also shown are NAB estimates (thin lines) with GC (blue) and AM3 (red). The grey band delineates the one standard deviation range about the observed regional mean monthly values.

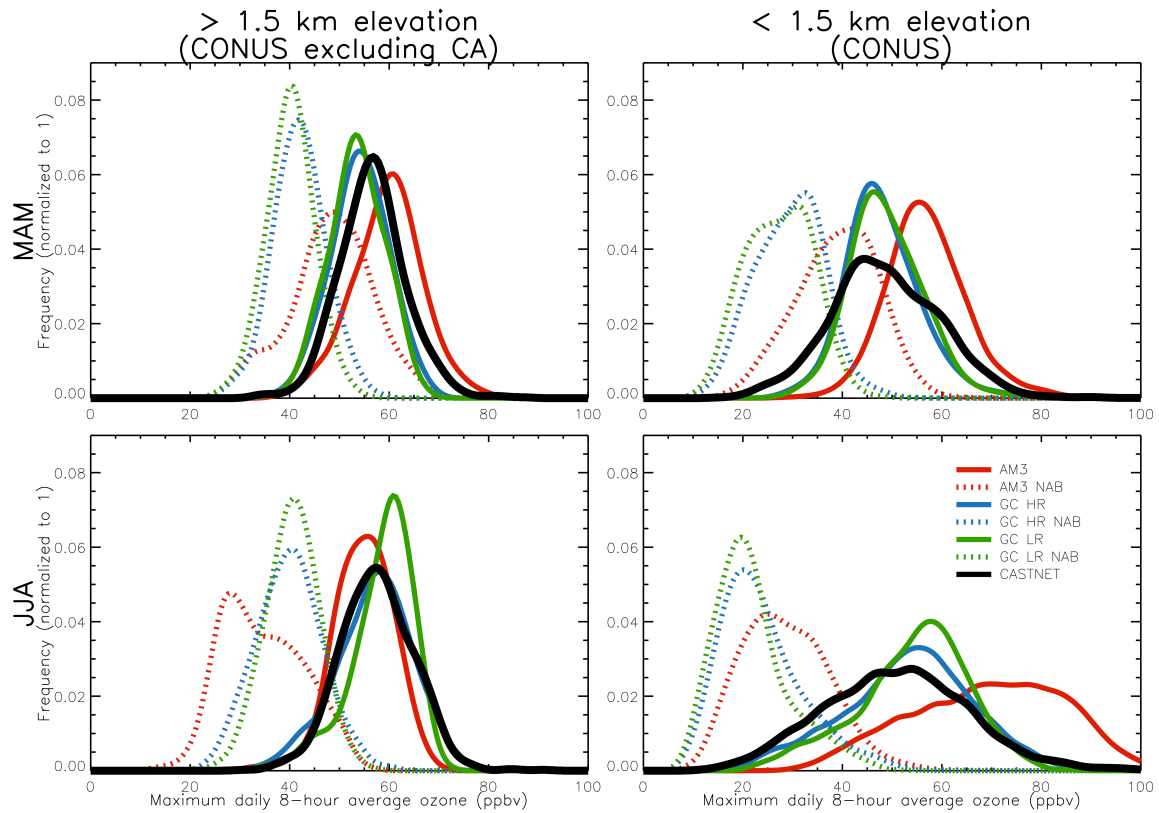


Figure 6. Probability density curves calculated via kernel (Gaussian) density estimation with a bandwidth of 2 ppbv from surface MDA8 O₃ data during spring (top) and summer (bottom) and at high (left, excluding California sites) and low (right) elevation CASTNet sites: observed (black) and GFDL AM3 (red) and GEOS-Chem at low (green; 2°x2.5°) and high (blue; 1/2° x 2/3°) horizontal resolution models sampled at the CASTNet sites for total (solid lines) and NAB (dashed lines) O₃.

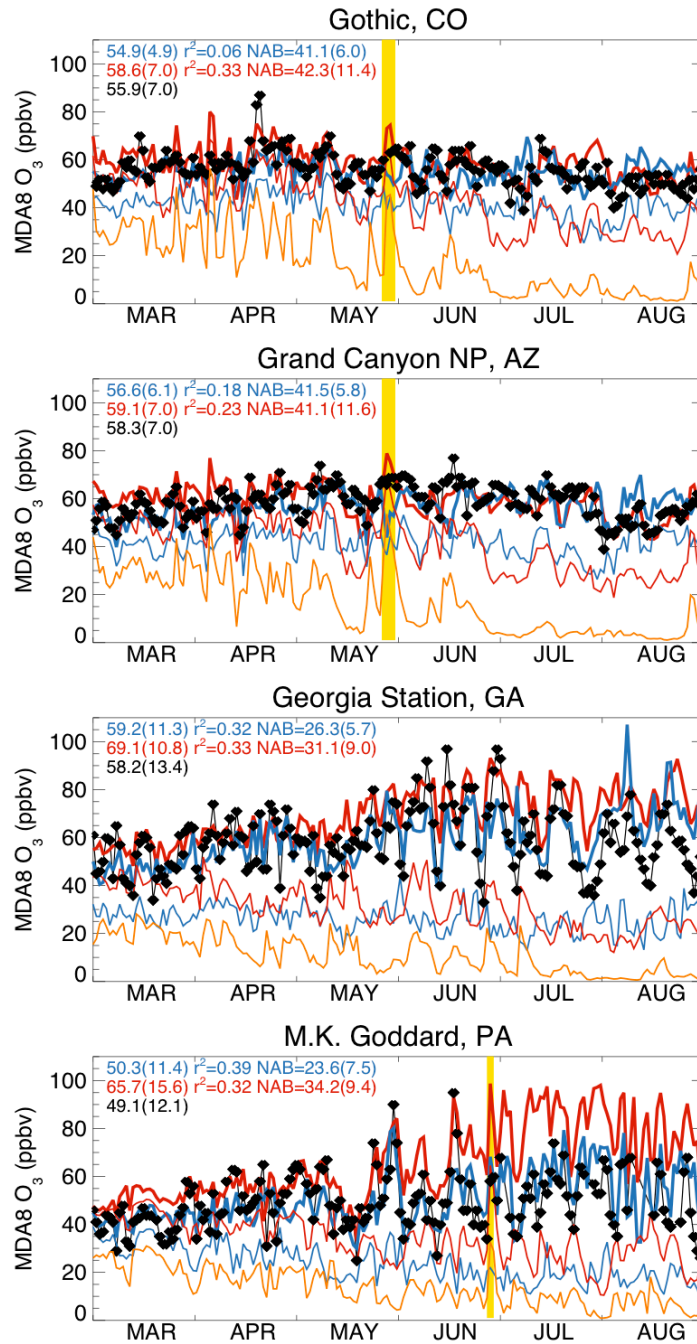


Figure 7. MDA8 O₃ in surface air observed (black) at four CASTNet sites for March through August 2006, and simulated with the GEOS-Chem (blue thick lines) and GFDL AM3 (red thick lines) models. Also shown are NAB estimates with GEOS-Chem (blue thin lines) and GFDL AM3 (red thin lines) and an estimate of stratospheric O₃ influence in the AM3 model (orange lines) following the method described in Lin et al. (2012b) from a simulation described in Lin et al. (2013). Statistics in the upper left corner of each panel are for the entire March through August period: the mean and standard deviation (in parentheses) of total surface O₃ as observed (black) and simulated with GEOS-Chem (blue) and GFDL AM3 (red); correlation coefficients of each model versus the

observations; the mean and standard deviation of the MDA8 NAB O₃ simulated with each model. Yellow highlighted days at the western U.S. sites and PA site correspond to case studies explored further in Figures 8-10 below. The Gothic, CO panel is Figure 3-75 of the U.S. EPA Integrated Science Assessment for O₃ (EPA, 2013).

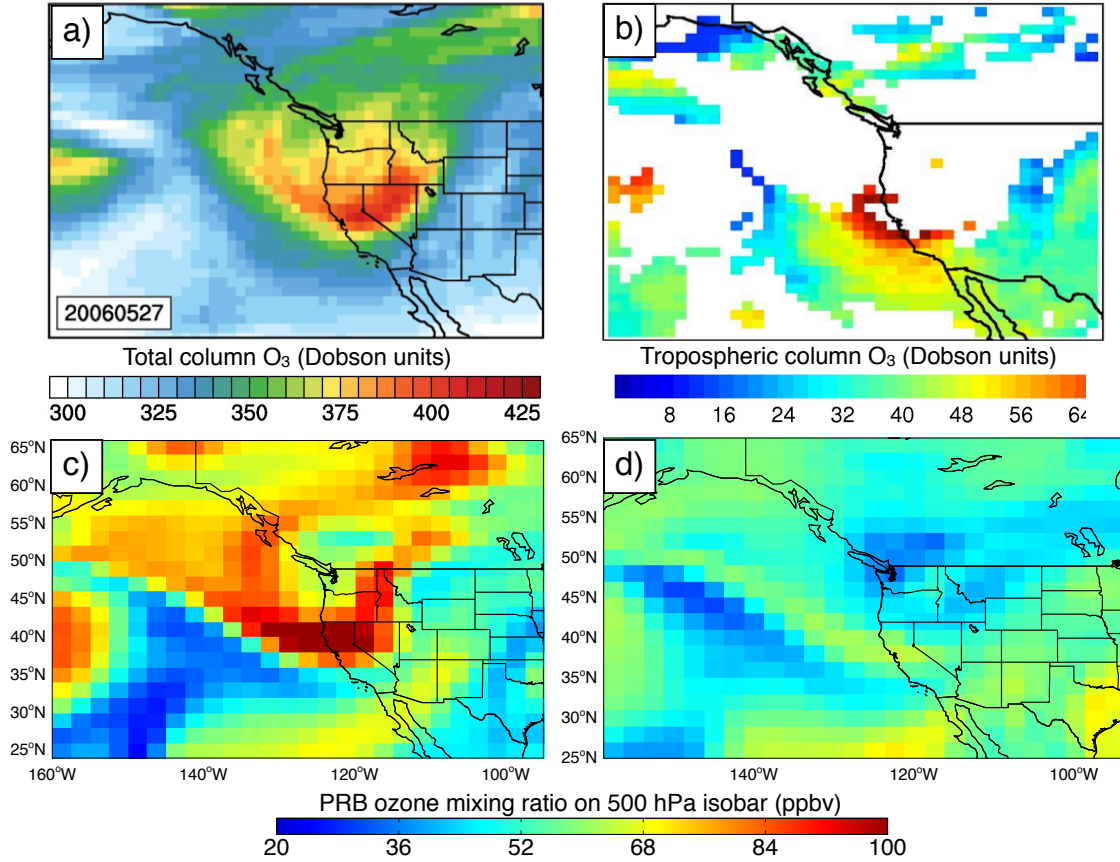


Figure 8. Snapshots of stratospheric ozone intrusion on May 27, 2006: a) Total column ozone from OMI, b) Tropospheric column ozone from OMI/MLS, and simulated 24-hour average 500 hPa NAB O₃ mixing ratios simulated with c) AM3 and d) coarse resolution GEOS-Chem (2°x2.5°).

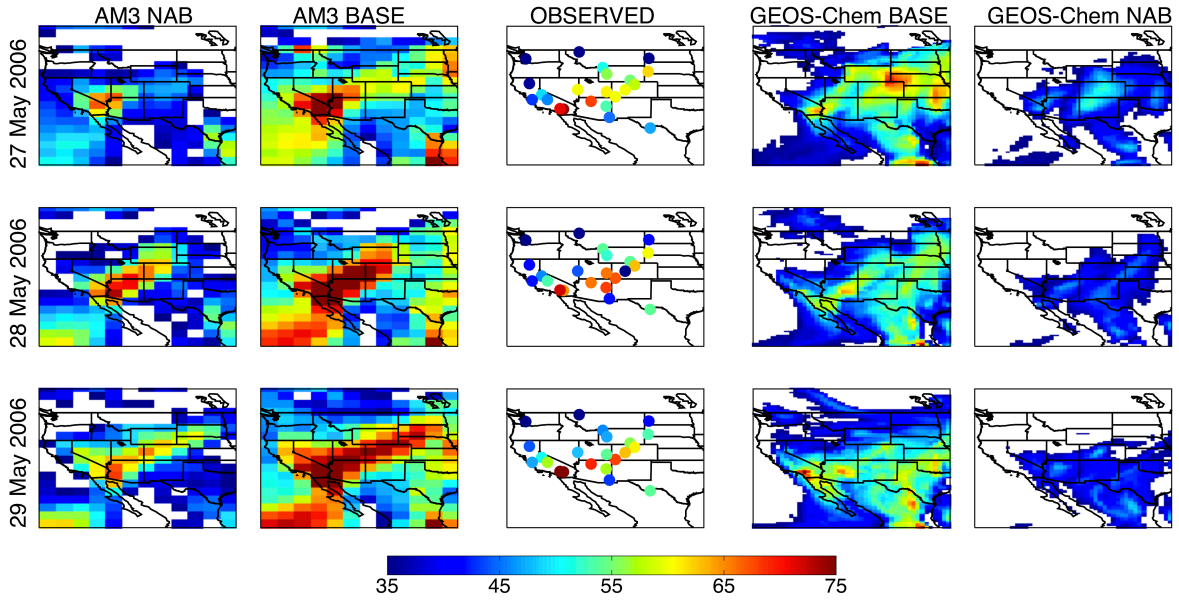


Figure 9: Surface O₃ over the Western U.S. associated with a stratospheric intrusion event on May 28, 2006. Shown are surface MDA8 O₃ on the days before (top), during (middle) and after (bottom) the event, as observed (center column) and as simulated by the AM3 model (second column) and GEOS-Chem (fourth column) models. Also shown is NAB MDA8 O₃ estimated in simulations with North American anthropogenic emissions set to zero in AM3 (first column) and GEOS-Chem (far right column).

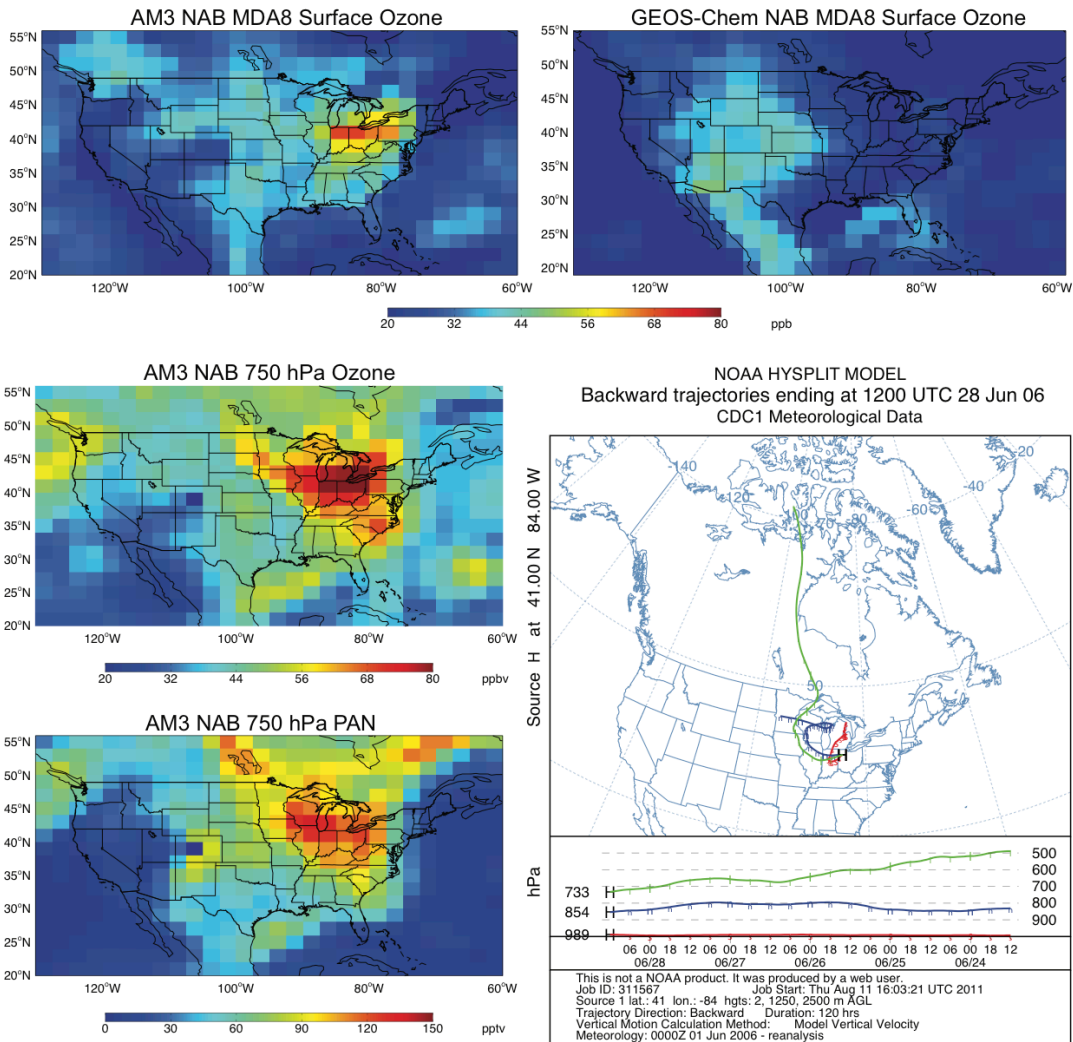


Figure 10. Illustrative example of model differences in NAB MDA8 O₃ events. Surface NAB MDA8 O₃, estimated with simulations in which North American anthropogenic emissions are set to zero, is shown for June 28, 2006 in AM3 (top left) and GEOS-Chem (top right). The high values over the Midwestern United States in the AM3 model are associated with enhanced O₃ (middle left) and PAN (middle left) at 750 hPa, attributed to biomass burning emissions over Canada and subsequent chemistry during transport along the back-trajectory shown (bottom right). See Section 3.4.2 for details.

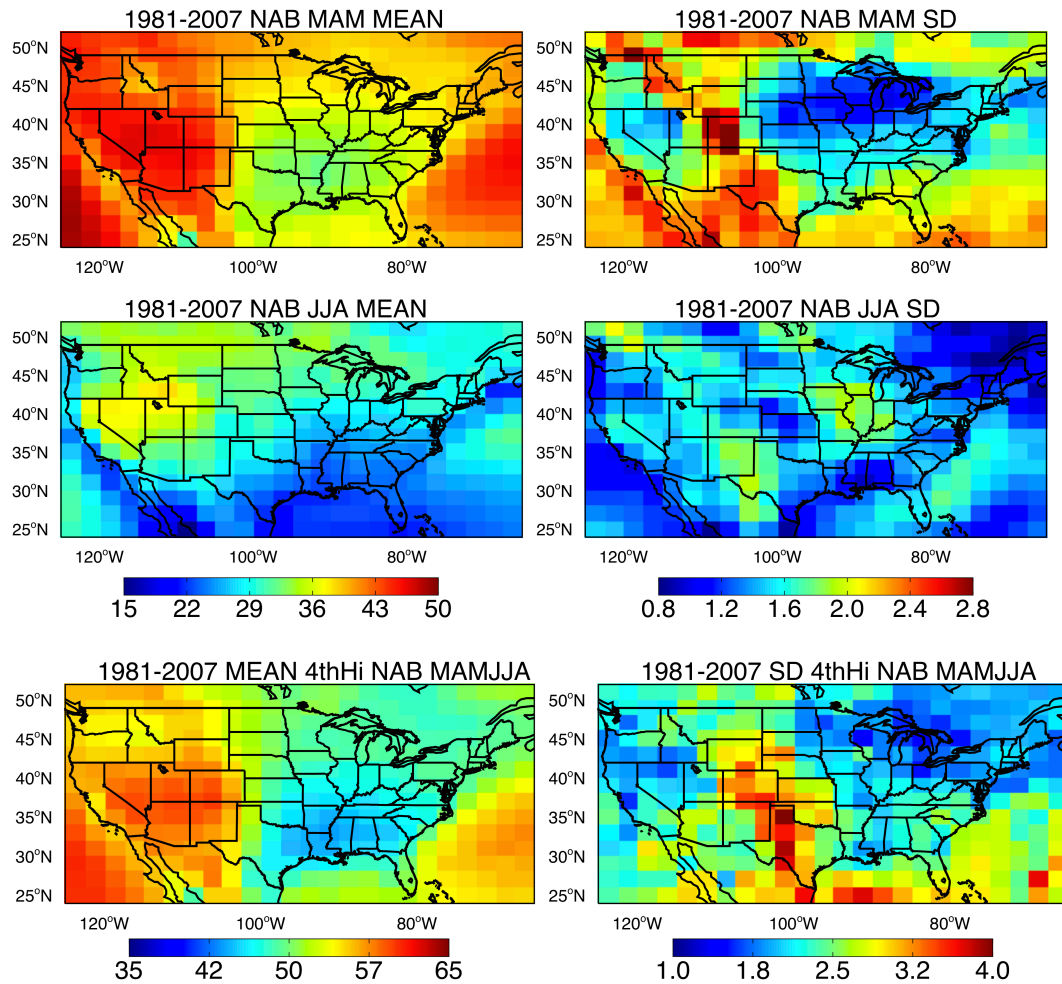


Figure 11. Climatological (1981-2007) average (left) and standard deviation (right) of spring (top) and summer (middle) seasonal mean MDA8 NAB O₃, and of the fourth highest value between March 1 and August 31 (bottom) as estimated with the GFDL AM3 model simulation in which North American anthropogenic emissions are set to zero.

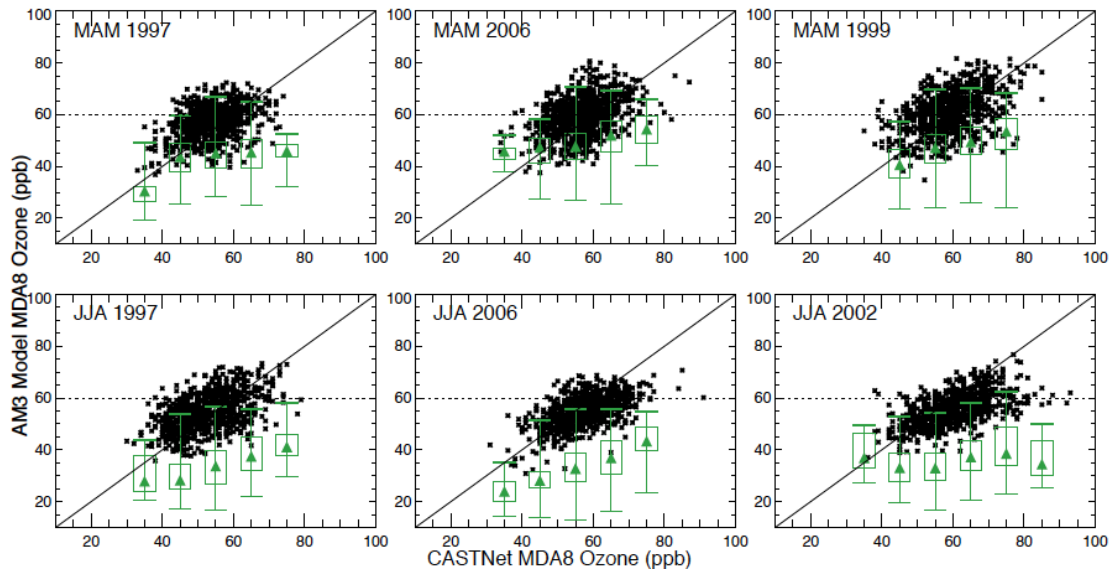


Figure 12. GFDL AM3 simulated daily maximum 8-hour (MDA8) surface O₃ versus observed values (black) and AM3 NAB statistics (green) at 11 Intermountain Western U.S. CASTNet sites above 1.5 km altitude for a “low-O₃” year (left column) and “high-O₃” year (right column) to provide context for the year 2006 (middle column) during spring (top panel) and summer (bottom panel), following the approach of Wang et al. (2009; see their Figure 5). The 1:1 line (solid black) and a 60 ppb threshold (dashed line) are shown. Box and whisker plots show the median (triangle), 25th-75th range (box) and minimum and maximum NAB values (vertical lines) for 10 ppb bins of observed O₃ values. The “low” and “high” years are selected from Figure 6 of Jaffe (2011).

References

- Baumgardner, R.E., Lavery, T.F., Rogers, C.M., Isil, S.S., 2002. Estimates of the Atmospheric Deposition of Sulfur and Nitrogen Species: The Clean Air Status and Trends Network, 1990-2000. *Environmental Science & Technology* 36, 2614-2629.
- Beer, R., 2006. TES on the aura mission: scientific objectives, measurements, and analysis overview. *Geoscience and Remote Sensing, IEEE Transactions on* 44, 1102-1105.
- Bey, I., Jacob, D.J., Yantosca, R.M., Logan, J.A., Field, B.D., Fiore, A.M., Li, Q., Liu, H.Y., Mickley, L.J., Schultz, M.G., 2001. Global modeling of tropospheric chemistry with assimilated meteorology: Model description and evaluation. *J. Geophys. Res.* 106, 23073-23095.
- Brown-Steiner, B., Hess, P., 2011. Asian influence on surface ozone in the United States: A comparison of chemistry, seasonality, and transport mechanisms. *J. Geophys. Res.* 116, D17309.
- Collins, W.J., Derwent, R.G., Garnier, B., Johnson, C.E., Sanderson, M.G., Stevenson, D.S., 2003. Effect of stratosphere-troposphere exchange on the future tropospheric ozone trend. *Journal of Geophysical Research: Atmospheres* 108, 8528.
- Cooper, O.R., Trainer, M., Thompson, A.M., Oltmans, S.J., Tarasick, D.W., Witte, J.C., Stohl, A., Eckhardt, S., Lelieveld, J., Newchurch, M.J., Johnson, B.J., Portmann, R.W., Kalnajs, L., Dubey, M.K., Leblanc, T., McDermid, I.S., Forbes, G., Wolfe, D., Carey-Smith, T., Morris, G.A., Lefer, B., Rappenglück, B., Joseph, E., Schmidlin, F., Meagher, J., Fehsenfeld, F.C., Keating, T.J., Van Curen, R.A., Minschwaner, K., 2007. Evidence for a recurring eastern North America upper tropospheric ozone maximum during summer. *Journal of Geophysical Research: Atmospheres* 112, D23304.
- Dentener, F., Kinne, S., Bond, T., Boucher, O., Cofala, J., Generoso, S., Ginoux, P., Gong, S., Hoelzemann, J.J., Ito, A., Marelli, L., Penner, J.E., Putaud, J.P., Textor, C., Schulz, M., van der Werf, G.R., Wilson, J., 2006. Emissions of primary aerosol and precursor gases in the years 2000 and 1750 prescribed data-sets for AeroCom. *Atmos. Chem. Phys.* 6, 4321-4344.
- Donner, L.J., Wyman, B.L., Hemler, R.S., Horowitz, L.W., Ming, Y., Zhao, M., Golaz, J.-C., Ginoux, P., Lin, S.J., Schwarzkopf, M.D., Austin, J., Alaka, G., Cooke, W.F., Delworth, T.L., Freidenreich, S.M., Gordon, C.T., Griffies, S.M., Held, I.M., Hurlin, W.J., Klein, S.A., Knutson, T.R., Langenhorst, A.R., Lee, H.-C., Lin, Y., Magi, B.I., Malyshev, S.L., Milly, P.C.D., Naik, V., Nath, M.J., Pincus, R., Ploshay, J.J., Ramaswamy, V., Seman, C.J., Shevliakova, E., Sirutis, J.J., Stern, W.F., Stouffer, R.J., Wilson, R.J., Winton, M., Wittenberg, A.T., Zeng, F., 2011. The Dynamical Core, Physical Parameterizations, and Basic Simulation Characteristics of the Atmospheric Component AM3 of the GFDL Global Coupled Model CM3. *Journal of Climate* 24, 3484-3519.
- Emery, C., Jung, J., Downey, N., Johnson, J., Jimenez, M., Yarwood, G., Morris, R., 2012. Regional and global modeling estimates of policy relevant background ozone over the United States. *Atmospheric Environment* 47, 206-217.

- Emmons, L.K., Walters, S., Hess, P.G., Lamarque, J.F., Pfister, G.G., Fillmore, D., Granier, C., Guenther, A., Kinnison, D., Laepple, T., Orlando, J., Tie, X., Tyndall, G., Wiedinmyer, C., Baughcum, S.L., Kloster, S., 2010. Description and evaluation of the Model for Ozone and Related chemical Tracers, version 4 (MOZART-4). *Geosci. Model Dev.* 3, 43-67.
- Federal Register, 2007. Environmental Protection Agency, 40 CFR Parts 50 and 51, Treatment of Data Influenced by Exceptional Events; Final Rule, pp. 13560-13581.
- Federal Register, 2010. National Ambient Air Quality Standards for Ozone, pp. 2938-3052.
- Fiore, A., Jacob, D.J., Liu, H., Yantosca, R.M., Fairlie, T.D., Li, Q., 2003. Variability in surface ozone background over the United States: Implications for air quality policy. *J. Geophys. Res.* 108, 4787.
- Fiore, A.M., Dentener, F.J., Wild, O., Cuvelier, C., Schultz, M.G., Hess, P., Textor, C., Schulz, M., Doherty, R.M., Horowitz, L.W., MacKenzie, I.A., Sanderson, M.G., Shindell, D.T., Stevenson, D.S., Szopa, S., Van Dingenen, R., Zeng, G., Atherton, C., Bergmann, D., Bey, I., Carmichael, G., Collins, W.J., Duncan, B.N., Faluvegi, G., Folberth, G., Gauss, M., Gong, S., Hauglustaine, D., Holloway, T., Isaksen, I.S.A., Jacob, D.J., Jonson, J.E., Kaminski, J.W., Keating, T.J., Lupu, A., Marnmer, E., Montanaro, V., Park, R.J., Pitari, G., Pringle, K.J., Pyle, J.A., Schroeder, S., Vivanco, M.G., Wind, P., Wojcik, G., Wu, S., Zuber, A., 2009. Multimodel estimates of intercontinental source-receptor relationships for ozone pollution. *J. Geophys. Res.* 114, D04301.
- Fiore, A.M., Horowitz, L.W., Purves, D.W., Levy, H., II, Evans, M.J., Wang, Y., Li, Q., Yantosca, R.M., 2005. Evaluating the contribution of changes in isoprene emissions to surface ozone trends over the eastern United States. *J. Geophys. Res.* 110, D12303.
- Fiore, A.M., Jacob, D.J., Bey, I., Yantosca, R.M., Field, B.D., Fusco, A.C., Wilkinson, J.G., 2002. Background ozone over the United States in summer: Origin, trend, and contribution to pollution episodes. *J. Geophys. Res.* 107, 4275.
- Guenther, A., Karl, T., Harley, P., Wiedinmyer, C., Palmer, P., Geron, C., 2006. Estimates of global terrestrial isoprene emissions using MEGAN (Model of Emissions of Gases and Aerosols from Nature). *Atmospheric Chemistry and Physics* 6, 3181-3210.
- Hilsenrath, E., Chance, K., 2013. NASA Ups the TEMPO on Monitoring Air Pollution. *The Earth Observer* 25, 10-15,35.
- Horowitz, L.W., Fiore, A.M., Milly, G.P., Cohen, R.C., Perring, A., Wooldridge, P.J., Hess, P.G., Emmons, L.K., Lamarque, J.-F., 2007. Observational constraints on the chemistry of isoprene nitrates over the eastern United States. *J. Geophys. Res.* 112, D12S08.
- Horowitz, L.W., Walters, S., Mauzerall, D.L., Emmons, L.K., Rasch, P.J., Granier, C., Tie, X., Lamarque, J.-F., Schultz, M.G., Tyndall, G.S., Orlando, J.J., Brasseur, G.P., 2003. A global simulation of tropospheric ozone and related tracers: Description and evaluation of MOZART, version 2. *J. Geophys. Res.* 108, 4784.
- Hudman, R.C., Jacob, D.J., Turquety, S., Leibensperger, E.M., Murray, L.T., Wu, S., Gilliland, A.B., Avery, M., Bertram, T.H., Brune, W., Cohen, R.C., Dibb, J.E.,

- Flocke, F.M., Fried, A., Holloway, J., Neuman, J.A., Orville, R., Perring, A., Ren, X., Sachse, G.W., Singh, H.B., Swanson, A., Wooldridge, P.J., 2007. Surface and lightning sources of nitrogen oxides over the United States: Magnitudes, chemical evolution, and outflow. *J. Geophys. Res.* 112, D12S05.
- Jacob, D.J., Horowitz, L.W., Munger, J.W., Heikes, B.G., Dickerson, R.R., Artz, R.S., Keene, W.C., 1995. Seasonal transition from NO_x- to hydrocarbon-limited conditions for ozone production over the eastern United States in September. *J. Geophys. Res.* 100, 9315-9324.
- Jaffe, D., 2011. Relationship between Surface and Free Tropospheric Ozone in the Western U.S. *Environmental Science & Technology* 45, 432-438.
- Jaffe, D.A., Wigder, N.L., 2012. Ozone production from wildfires: A critical review. *Atmospheric Environment* 51, 1-10.
- Kalnay, E., Kanamitsu, M., Kistler, R., Collins, W., Deaven, D., Gandin, L., Iredell, M., Saha, S., White, G., Woollen, J., Zhu, Y., Leetmaa, A., Reynolds, R., Chelliah, M., Ebisuzaki, W., Higgins, W., Janowiak, J., Mo, K.C., Ropelewski, C., Wang, J., Jenne, R., Joseph, D., 1996. The NCEP/NCAR 40-Year Reanalysis Project. *Bulletin of the American Meteorological Society* 77, 437-471.
- Kaynak, B., Hu, Y., Martin, R.V., Russell, A.G., Choi, Y., Wang, Y., 2008. The effect of lightning NO_x production on surface ozone in the continental United States. *Atmos. Chem. Phys.* 8, 5151-5159.
- Lamarque, J.-F., Kyle, G., Meinshausen, M., Riahi, K., Smith, S., van Vuuren, D., Conley, A., Vitt, F., 2011. Global and regional evolution of short-lived radiatively-active gases and aerosols in the Representative Concentration Pathways. *Climatic Change* 109, 1-22.
- Lamarque, J.F., Bond, T.C., Eyring, V., Granier, C., Heil, A., Klimont, Z., Lee, D., Liousse, C., Mieville, A., Owen, B., Schultz, M.G., Shindell, D., Smith, S.J., Stehfest, E., Van Aardenne, J., Cooper, O.R., Kainuma, M., Mahowald, N., McConnell, J.R., Naik, V., Riahi, K., van Vuuren, D.P., 2010. Historical (1850-2000) gridded anthropogenic and biomass burning emissions of reactive gases and aerosols: methodology and application. *Atmos. Chem. Phys.* 10, 7017-7039.
- Langford, A.O., Aikin, K.C., Eubank, C.S., Williams, E.J., 2009. Stratospheric contribution to high surface ozone in Colorado during springtime. *Geophys. Res. Lett.* 36, L12801.
- Lin, M., Fiore, A.M., Cooper, O.R., Horowitz, L.W., Langford, A.O., Levy, H., Johnson, B.J., Naik, V., Oltmans, S.J., Senff, C.J., 2012a. Springtime high surface ozone events over the western United States: Quantifying the role of stratospheric intrusions. *Journal of Geophysical Research: Atmospheres* 117, D00V22.
- Lin, M., Fiore, A.M., Horowitz, L.W., Cooper, O.R., Naik, V., Holloway, J., Johnson, B.J., Middlebrook, A.M., Oltmans, S.J., Pollack, I.B., Ryerson, T.B., Warner, J.X., Wiedinmyer, C., Wilson, J., Wyman, B., 2012b. Transport of Asian ozone pollution into surface air over the western United States in spring. *J. Geophys. Res.* 117, D00V07.
- Lin, M., L.W. Horowitz, Oltmans, S.J., Fiore, A.M., Fan, S., 2013. Tropospheric ozone trends at Mauna Loa Observatory tied to decadal climate variability. *Nature Geoscience*, in press.

- Liu, X., Bhartia, P.K., Chance, K., Spurr, R.J.D., Kurosu, T.P., 2010. Ozone profile retrievals from the Ozone Monitoring Instrument. *Atmos. Chem. Phys.* 10, 2521-2537.
- Mao, J., Paulot, F., Jacob, D.J., Cohen, R.C., Crouse, J.D., Wennberg, P.O., Keller, C.A., Hudman, R.C., Barkley, M.P., Horowitz, L.W., 2013. Ozone and organic nitrates over the eastern United States: Sensitivity to isoprene chemistry. *Journal of Geophysical Research: Atmospheres*, n/a-n/a.
- Martin, R.V., Sauvage, B., Folkins, I., Sioris, C.E., Boone, C., Bernath, P., Ziemke, J., 2007. Space-based constraints on the production of nitric oxide by lightning. *J. Geophys. Res.* 112, D09309.
- McDonald-Buller, E.C., Allen, D.T., Brown, N., Jacob, D.J., Jaffe, D., Kolb, C.E., Lefohn, A.S., Oltmans, S., Parrish, D.D., Yarwood, G., Zhang, L., 2011. Establishing Policy Relevant Background (PRB) Ozone Concentrations in the United States. *Environmental Science & Technology* 45, 9484-9497.
- McKeen, S.A., Wotawa, G., Parrish, D.D., Holloway, J.S., Buhr, M.P., Hübler, G., Fehsenfeld, F.C., Meagher, J.F., 2002. Ozone production from Canadian wildfires during June and July of 1995. *Journal of Geophysical Research: Atmospheres* 107, ACH 7-1-ACH 7-25.
- McLinden, C.A., Olsen, S.C., Hannegan, B., Wild, O., Prather, M.J., Sundet, J., 2000. Stratospheric ozone in 3-D models: A simple chemistry and the cross-tropopause flux. *J. Geophys. Res.* 105, 14653-14665.
- Mickley, L.J., Jacob, D.J., Rind, D., 2001. Uncertainty in preindustrial abundance of tropospheric ozone: Implications for radiative forcing calculations. *J. Geophys. Res.* 106, 3389-3399.
- Mueller, S.F., Mallard, J.W., 2011. Contributions of Natural Emissions to Ozone and PM_{2.5} as Simulated by the Community Multiscale Air Quality (CMAQ) Model. *Environmental Science & Technology* 45, 4817-4823.
- Murray, L.T., Jacob, D.J., Logan, J.A., Hudman, R.C., Koshak, W.J., 2012. Optimized regional and interannual variability of lightning in a global chemical transport model constrained by LIS/OTD satellite data. *Journal of Geophysical Research: Atmospheres* 117, D20307.
- Naik, V., Horowitz, L.W., Fiore, A.M., Ginoux, P., Mao, J., Aghedo, A.M., Levy, H., 2013. Impact of preindustrial to present-day changes in short-lived pollutant emissions on atmospheric composition and climate forcing. *Journal of Geophysical Research: Atmospheres* 118, 8086-8110.
- Olivier, J.G.J., Berdowski, J.J.M., 2001. Global emissions sources and sinks, in: *The Climate System*, in: Berdowski, J., Guicherit, R., Heij, B.J. (Eds.), Lisse, The Netherlands, pp. 33-78.
- Park, R.J., Jacob, D.J., Field, B.D., Yantosca, R.M., Chin, M., 2004. Natural and transboundary pollution influences on sulfate-nitrate-ammonium aerosols in the United States: Implications for policy. *Journal of Geophysical Research: Atmospheres* 109, D15204.
- Parrella, J.P., Jacob, D.J., Liang, Q., Zhang, Y., Mickley, L.J., Miller, B., Evans, M.J., Yang, X., Pyle, J.A., Theys, N., Van Roozendaal, M., 2012. Tropospheric bromine chemistry: implications for present and pre-industrial ozone and mercury. *Atmos. Chem. Phys.* 12, 6723-6740.

- Perring, A.E., Bertram, T.H., Wooldridge, P.J., Fried, A., Heikes, B.G., Dibb, J., Crouse, J.D., Wennberg, P.O., Blake, N.J., Blake, D.R., Brune, W.H., Singh, H.B., Cohen, R.C., 2009. Airborne observations of total RONO₂: New constraints on the yield and lifetime of isoprene nitrates. *Atmospheric Chemistry and Physics* 9, 1451-1463.
- Prather, M.J., Zhu, X., Tang, Q., Hsu, J., Neu, J.L., 2011. An atmospheric chemist in search of the tropopause. *J. Geophys. Res.* 116, D04306.
- Price, C., Rind, D., 1992. A simple lightning parameterization for calculating global lightning distributions. *Journal of Geophysical Research: Atmospheres* 97, 9919-9933.
- Rasmussen, D.J., Fiore, A.M., Naik, V., Horowitz, L.W., McGinnis, S.J., Schultz, M.G., 2012. Surface ozone-temperature relationships in the eastern US: A monthly climatology for evaluating chemistry-climate models. *Atmospheric Environment* 47, 142-153.
- Reid, N., Yap, D., Bloxam, R., 2008. The potential role of background ozone on current and emerging air issues: An overview. *Air Qual Atmos Health* 1, 19-29.
- Reidmiller, D.R., Fiore, A.M., Jaffe, D.A., Bergmann, D., Cuvelier, C., Dentener, F.J., Duncan, B.N., Folberth, G., Gauss, M., Gong, S., Hess, P., Jonson, J.E., Keating, T., Lupu, A., Marmer, E., Park, R., Schultz, M.G., Shindell, D.T., Szopa, S., Vivanco, M.G., Wild, O., Zuber, A., 2009. The influence of foreign vs. North American emissions on surface ozone in the US. *Atmos. Chem. Phys.* 9, 5027-5042.
- Singh, H.B., Anderson, B.E., Brune, W.H., Cai, C., Cohen, R.C., Crawford, J.H., Cubison, M.J., Czech, E.P., Emmons, L., Fuelberg, H.E., Huey, G., Jacob, D.J., Jimenez, J.L., Kaduwela, A., Kondo, Y., Mao, J., Olson, J.R., Sachse, G.W., Vay, S.A., Weinheimer, A., Wennberg, P.O., Wisthaler, A., 2010. Pollution influences on atmospheric composition and chemistry at high northern latitudes: Boreal and California forest fire emissions. *Atmospheric Environment* 44, 4553-4564.
- Task Force on Hemispheric Transport of Air Pollution (TF HTAP), 2010. HEMISPHERIC TRANSPORT OF AIR POLLUTION 2010 PART A: OZONE AND PARTICULATE MATTER, Air Pollution Studies No. 17, in: Dentener, F., Keating, T., Akimoto, H. (Eds.), AIR POLLUTION STUDIES No. 17. UNITED NATIONS, New York.
- U.S. EPA, 2006. Air Quality Criteria for Ozone and Related Photochemical Oxidants (2006 Final). in: Agency, U.S.E.P. (Ed.), Washington, DC.
- U.S. EPA, 2013. Integrated Science Assessment of Ozone and Related Photochemical Oxidants (Final Report). in: Agency, U.S.E.P. (Ed.), Washington, DC.
- van der Werf, G.R., Randerson, J.T., Giglio, L., Collatz, G.J., Kasibhatla, P.S., Arellano Jr, A.F., 2006. Interannual variability in global biomass burning emissions from 1997 to 2004. *Atmos. Chem. Phys.* 6, 3423-3441.
- Vingarzan, R., 2004. A review of surface ozone background levels and trends. *Atmospheric Environment* 38, 3431-3442.
- Wang, H., Jacob, D.J., Le Sager, P., Streets, D.G., Park, R.J., Gilliland, A.B., van Donkelaar, A., 2009. Surface ozone background in the United States: Canadian and Mexican pollution influences. *Atmospheric Environment* 43, 1310-1319.

- Wang, Y.X., McElroy, M.B., Jacob, D.J., Yantosca, R.M., 2004. A nested grid formulation for chemical transport over Asia: Applications to CO. *Journal of Geophysical Research: Atmospheres* 109, D22307.
- Wild, O., Fiore, A.M., Shindell, D.T., Doherty, R.M., Collins, W.J., Dentener, F.J., Schultz, M.G., Gong, S., MacKenzie, I.A., Zeng, G., Hess, P., Duncan, B.N., Bergmann, D.J., Szopa, S., Jonson, J.E., Keating, T.J., Zuber, A., 2012. Modelling future changes in surface ozone: a parameterized approach. *Atmos. Chem. Phys.* 12, 2037-2054.
- Wu, S., Mickley, L.J., Jacob, D.J., Rind, D., Streets, D.G., 2008. Effects of 2000-2050 changes in climate and emissions on global tropospheric ozone and the policy-relevant background surface ozone in the United States. *J. Geophys. Res.* 113, D18312.
- Zhang, L., Jacob, D.J., Boersma, K.F., Jaffe, D.A., Olson, J.R., Bowman, K.W., Worden, J.R., Thompson, A.M., Avery, M.A., Cohen, R.C., Dibb, J.E., Flocke, F.M., Fuelberg, H.E., Huey, L.G., McMillian, W.W., Singh, H.B., Weinheimer, A.J., 2008. Transpacific transport of ozone pollution and the effect of recent Asian emission increases on air quality in North America: an integrated analysis using satellite, aircraft, ozonesonde, and surface observations. *Atmospheric Chemistry and Physics* 8, 6117-6136.
- Zhang, L., Jacob, D.J., Downey, N.V., Wood, D.A., Blewitt, D., Carouge, C.C., van Donkelaar, A., Jones, D.B.A., Murray, L.T., Wang, Y., 2011. Improved estimate of the policy-relevant background ozone in the United States using the GEOS-Chem global model with $\frac{1}{2}^{\circ} \times \frac{2}{3}^{\circ}$ horizontal resolution over North America. *Atmospheric Environment* 45, 6769-6776.
- Zhang, L., Jacob, D.J., Liu, X., Logan, J.A., Chance, K., Eldering, A., Bojkov, B.R., 2010. Intercomparison methods for satellite measurements of atmospheric composition: application to tropospheric ozone from TES and OMI. *Atmos. Chem. Phys.* 10, 4725-4739.
- Zhang, L., Jacob, D.J., Yue, X., Downey, N.V., Wood, D.A., Blewitt, D., 2013. Sources contributing to background surface ozone in the US Intermountain West. *Atmos. Chem. Phys. Discuss.* 13, 25871-25909.